

# RSC Advances



This article can be cited before page numbers have been issued, to do this please use: B. Maleki, M. Baghayeri, S. Ayazi Jannat Abadi, R. Tayebbe and A. Khojastehnezhad, *RSC Adv.*, 2016, DOI: 10.1039/C6RA20895A.



This is an *Accepted Manuscript*, which has been through the Royal Society of Chemistry peer review process and has been accepted for publication.

*Accepted Manuscripts* are published online shortly after acceptance, before technical editing, formatting and proof reading. Using this free service, authors can make their results available to the community, in citable form, before we publish the edited article. This *Accepted Manuscript* will be replaced by the edited, formatted and paginated article as soon as this is available.

You can find more information about *Accepted Manuscripts* in the [Information for Authors](#).

Please note that technical editing may introduce minor changes to the text and/or graphics, which may alter content. The journal's standard [Terms & Conditions](#) and the [Ethical guidelines](#) still apply. In no event shall the Royal Society of Chemistry be held responsible for any errors or omissions in this *Accepted Manuscript* or any consequences arising from the use of any information it contains.

# Ultrasound Promoted Facile One Pot Synthesis of Highly Substituted Pyran Derivatives Catalyzed by Silica-Coated Magnetic NiFe<sub>2</sub>O<sub>4</sub> Nanoparticles-Supported H<sub>14</sub>[NaP<sub>5</sub>W<sub>30</sub>O<sub>110</sub>] under Mild Conditions

Behrooz Maleki<sup>\*1</sup>, Mehdi Baghayeri<sup>1</sup>, Sedigheh Ayazi Jannat Abadi<sup>1</sup>, Reza Tayebee<sup>1</sup> and Amir Khojastehnezhad<sup>2</sup>

<sup>1</sup>Department of Chemistry, Hakim Sabzevari University, Sabzevar, 96179-76487, Iran

E-mail: malekibehrooz@gmail.com, Tel: +98-44013324

<sup>2</sup>Young Researchers and Elite Club, Mashhad Branch, Islamic Azad University, Mashhad, Iran

## Abstract

Silica-coated magnetic NiFe<sub>2</sub>O<sub>4</sub> nanoparticles-supported Preyssler heteropolyacid (H<sub>14</sub>[NaP<sub>5</sub>W<sub>30</sub>O<sub>110</sub>]) catalyzed efficiently the synthesis of highly substituted pyran derivatives under ultrasonic irradiation at room temperature in ethanol. In comparison with conventional methods, our protocol is convenient and offers several advantages, such as shorter reaction times, higher yields, milder conditions and environmental friendliness. The catalyst can be recovered by a simple external magnet and used for four times without a significant loss of catalytic activity.

**Keywords:** Ultrasonic radiation; NiFe<sub>2</sub>O<sub>4</sub>@SiO<sub>2</sub>-H<sub>14</sub>[NaP<sub>5</sub>W<sub>30</sub>O<sub>110</sub>]; One-pot synthesis; magnetically retrievable catalyst; Highly substituted pyrans

## Introduction

Use of ultrasound as a means of accelerating reactions has long been known in both industry and academia. Considering the basic green chemistry concepts, ultrasound technique is being proved to be an important tool in the arsenal of “Green Chemistry”. The use of ultrasound for improving the traditional reactions that require longer reaction time, unsatisfactory yields, expensive reagents and high temperature is commonly termed as sonochemistry. The sonochemistry is a simple, novel and powerful tool for the synthesis of organic compounds and nanoparticles at low temperature. The chemical and physical effects of ultrasound come from acoustic cavitations such as the formation, growth and implosive collapse of bubbles in a liquid. The cavitation collapse creates drastic conditions inside the medium for an extremely short time and temperature of 2000-5000 K as well as pressure upto 1800 atm inside the collapsing cavity have been produced under sonic conditions. The cavitation effect produces effective physical, chemical and biological transformations. Thus ultrasound has applications in material sciences, life sciences and medicine.<sup>1-4</sup>

Recently, multi-component reactions (MCRs) have received much attention in the field of synthetic organic chemistry as well as medicinal chemistry, because the strategies of MCR offer significant advantages over conventional synthetic methodologies. This ensures high atom economy, good yields and low costs, in short reaction times, minimization of waste, labor, energy, and avoidance of tedious purification processes.<sup>5-8</sup>

Nanomagnetic catalysts are one of the most promising areas in organic synthesis and it has gained considerable attention in recent times. In this aspect synthesis and use of magnetic nanoparticles has gained significant attention among academic and industrial community because

are non-toxic, inexpensive, easily available, recyclable and show significant enhancement in catalytic activity due to small size, high surface area, active sites. Moreover, these magnetic nanoparticles can be effectively recovered after completion of reaction, without any loss, which is the drawback of traditional methods like centrifugation and filtration.<sup>9-10</sup> Similarly, MCRs are a popular and greener synthetic tool to access diverse molecular scaffolds. Combining both concepts, nanomagnetic catalyst in MCRs has emerged as a very useful strategy in organic synthesis.<sup>11-13</sup>

In continuation of our research work on MCRs,<sup>14-21</sup> we were interested to explore the catalytic potential of silica-coated magnetic NiFe<sub>2</sub>O<sub>4</sub> nanoparticles-supported H<sub>14</sub>[NaP<sub>5</sub>W<sub>30</sub>O<sub>110</sub>] (abbreviated NFS-PRS) in our MCRs for easy access to diverse and highly substituted pyrans. From the literature studies we realized that highly substituted pyrans (tetrahydrobenzo[b]pyrans, 2-amino-3-cyano-4H-pyrans, and pyrano [2, 3-c]pyrazoles) tethered with -NH<sub>2</sub> and -CN functionality in the 2,3-position, as shown as in Fig. 1, possesses diverse pharmacological properties.

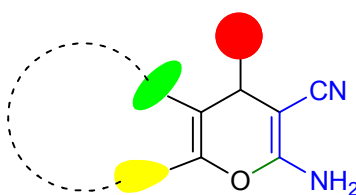


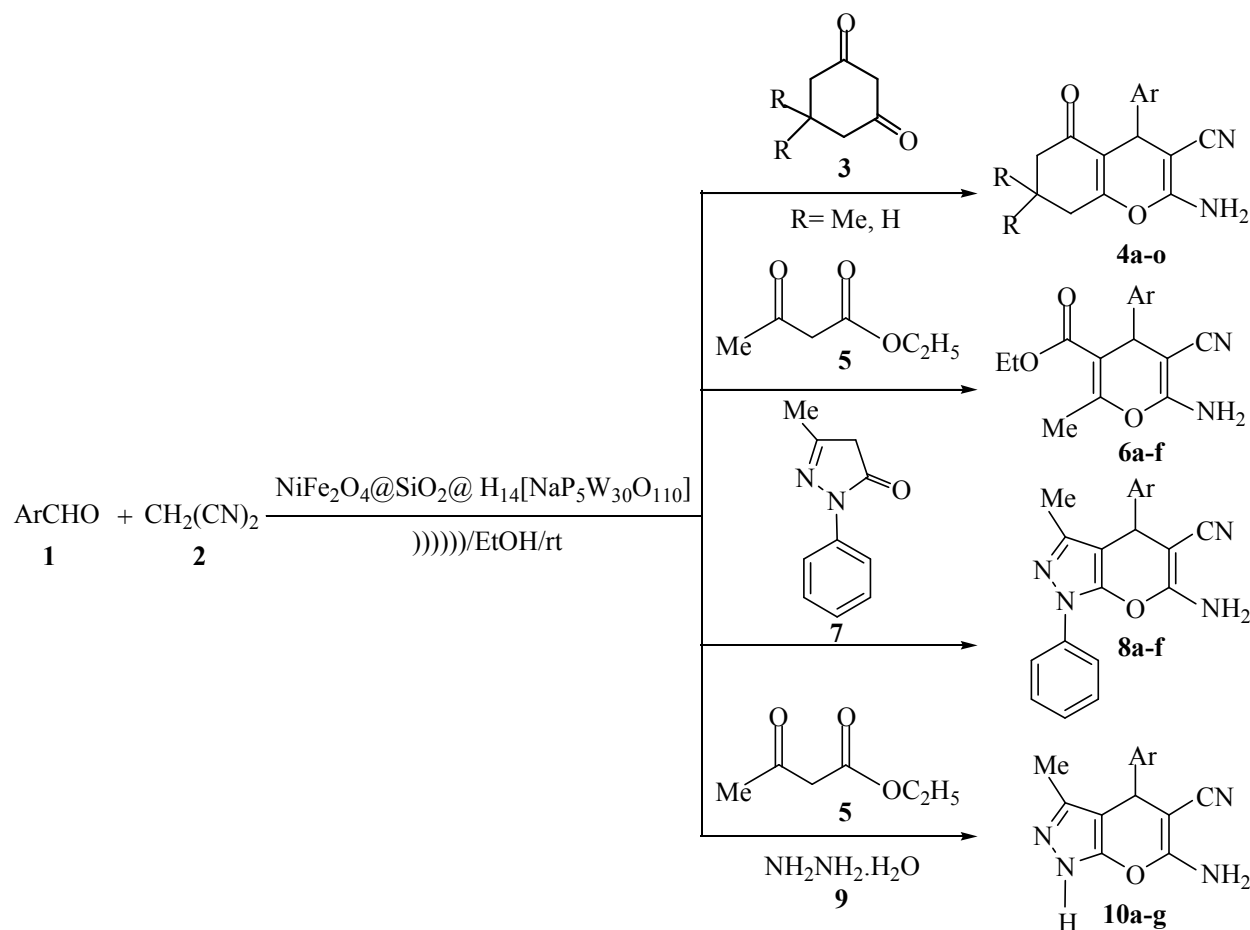
**Fig 1.** Core of highly substituted 4H-pyrans with amino and nitrile functionality in the adjacent position having diverse pharmacological properties

Compounds bearing a pyran framework are found to possess unique, valuable medicinal properties and play crucial roles in biochemical processes.<sup>22-23</sup> Amongst the humongous scaffold, 4*H*-pyran and its derivatives have occupied a distinctive place in the field of medicinal chemistry towards the design of biologically active compounds.<sup>24-27</sup> They possess varied pharmacological activities such as antibacterial,<sup>28</sup> spasmolytic, anticoagulant, diuretic<sup>29</sup> activity, antitumor,<sup>30</sup> Anti-Inflammatory,<sup>31</sup> anti HIV, analgesic and myorelaxant<sup>32</sup> activities. These compounds have been an asset in combating Schizophrenia, Alzheimer and mycolonous diseases.<sup>33</sup> Additionally, 4*H*-pyrans find their utility in biodegradable agrochemicals, pigments, cosmetics, photoactive materials and fluorescent reagents.<sup>34-35</sup>

Considering their importance, a considerable number of methods are found in the literature for the synthesis of these molecules.<sup>36-55</sup> Although a wide range of methods exist in the literature, still better and more efficient methods that provide easy access to these functionalized molecules are sought after due to the diverse biological applications of these molecules.

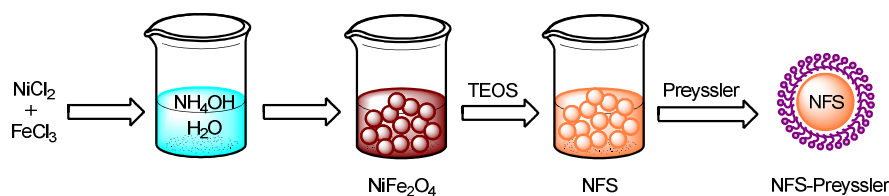
## Results and discussion

In this research, we combined the advantages of ultrasonic irradiation and nanotechnology to find the more convenient and efficient reaction of highly substituted pyrans (tetrahydrobenzo[b]pyrans, 2-amino-3-cyano-4*H*-pyrans, and pyrano [2, 3-*c*]pyrazoles) (Scheme 1).



**Scheme 1.** One-pot synthesis of highly substituted pyran derivatives

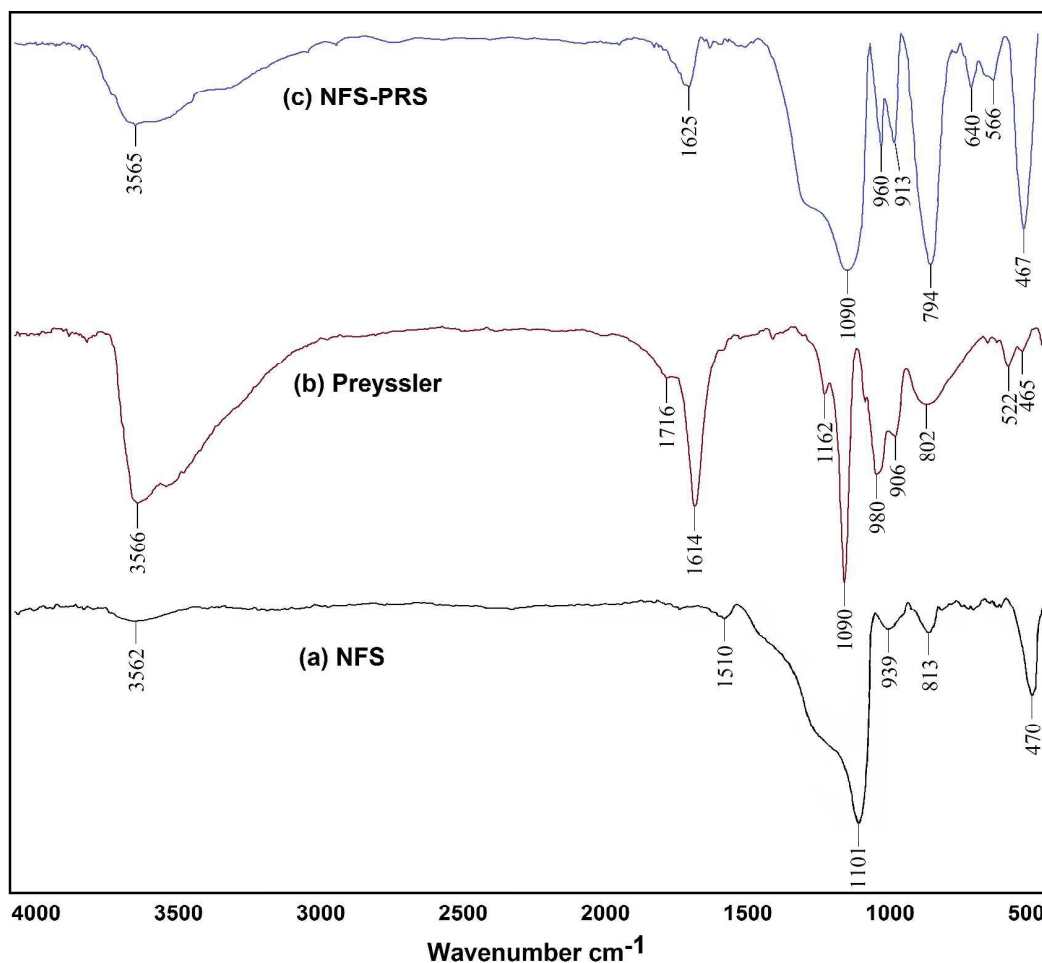
A synthetic strategy of silica-coated magnetic  $\text{NiFe}_2\text{O}_4$  nanoparticle supported  $\text{H}_{14}[\text{NaP}_5\text{W}_{30}\text{O}_{110}]$  ( $\text{NiFe}_2\text{O}_4@\text{SiO}_2-\text{H}_{14}[\text{NaP}_5\text{W}_{30}\text{O}_{110}]$ ) is shown in the Fig. 2. At first, silica-coated magnetic  $\text{NiFe}_2\text{O}_4$  nanoparticle ( $\text{NiFe}_2\text{O}_4@\text{SiO}_2$ ) was prepared according to our previous reports.<sup>56-58</sup> The  $\text{NiFe}_2\text{O}_4@\text{SiO}_2$  was treated with  $\text{H}_{14}[\text{NaP}_5\text{W}_{30}\text{O}_{110}]$  to yield  $\text{NiFe}_2\text{O}_4@\text{SiO}_2-\text{H}_{14}[\text{NaP}_5\text{W}_{30}\text{O}_{110}]$ . The catalyst was characterized using various methods.



TEOS = Tetraethylorthosilicate, Preyssler =  $H_{14}[NaP_5W_{30}O_{110}]$   
 NFS-PRS =  $NiFe_2O_4@SiO_2-H_{14}[NaP_5W_{30}O_{110}]$

**Fig 2.** Preparation of  $NiFe_2O_4@SiO_2-H_{14}[NaP_5W_{30}O_{110}]$

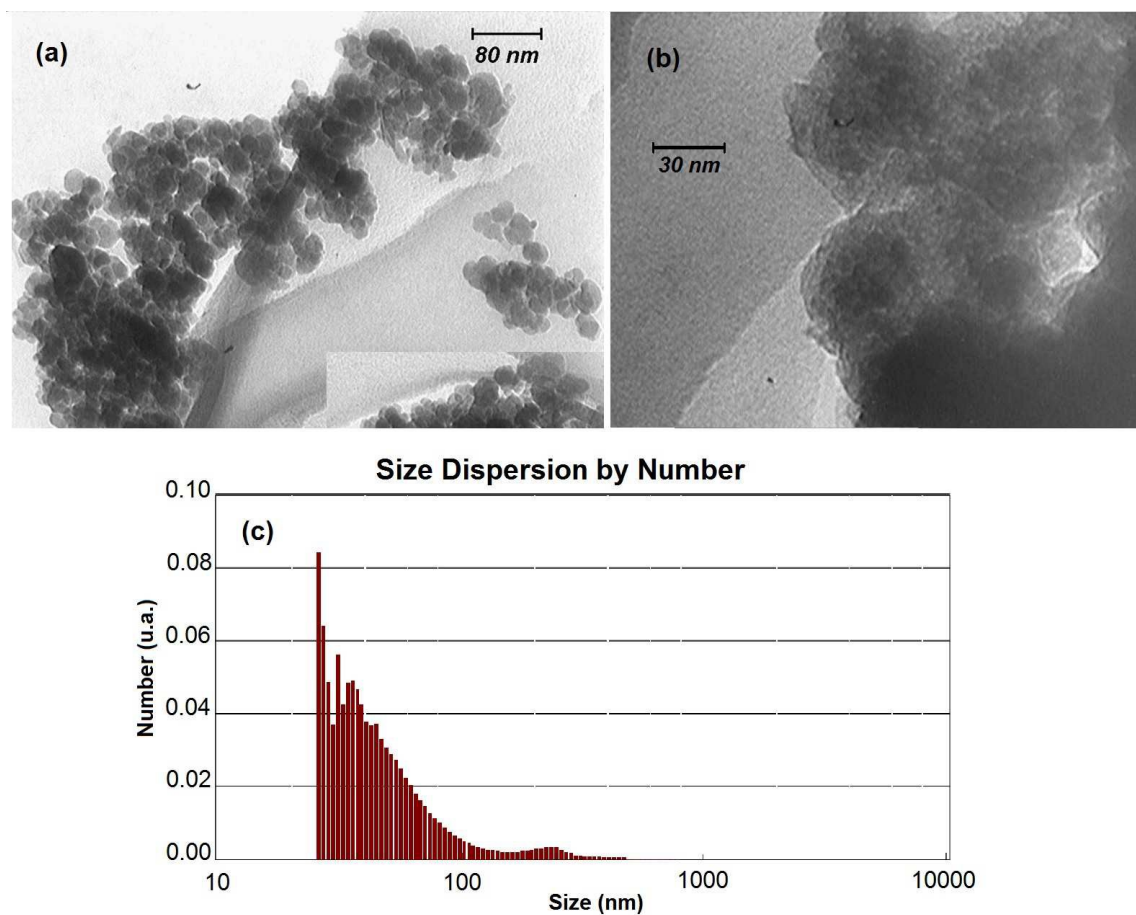
The FT-IR spectra of  $NiFe_2O_4@SiO_2$  (NFS), Preyssler ( $H_{14}[NaP_5W_{30}O_{110}]$ ) and  $NiFe_2O_4@SiO_2-H_{14}[NaP_5W_{30}O_{110}]$  (NFS-PRS) are compared in Fig. 3. The FT-IR spectrum of  $NiFe_2O_4@SiO_2$  (Fig. 3a) exhibits high intense absorption peak  $1101\text{ cm}^{-1}$  and this peak is assigned to the longitudinal and transverse stretching vibration modes of the Si–O–Si asymmetric bond respectively. Additional bands at  $813\text{ cm}^{-1}$  and  $470\text{ cm}^{-1}$  are also identified as the characteristic peaks of Si–O–Si bond respectively. The other peak observed at  $939\text{ cm}^{-1}$  assigned to the  $SiO_3^{-2}$  vibrations indicates the existence of nonbridging oxygen ions.<sup>59-60</sup> The spectrum of  $H_{14}[NaP_5W_{30}O_{110}]$  (Fig. 3b) displayed vibrations at  $1,162$  and  $1,090\text{ cm}^{-1}$  for P–O stretching in  $H_{14}[NaP_5W_{30}O_{110}]$  structure,  $980$  and  $906\text{ cm}^{-1}$  for W–O–W stretching,  $802\text{ cm}^{-1}$  for W=O stretching, and  $522\text{ cm}^{-1}$  for P–O bending,<sup>61</sup> also there is a high intense absorption peak around  $1614\text{ cm}^{-1}$ , which was attributed to adsorbed water.<sup>62</sup> In the FT-IR spectrum of  $NiFe_2O_4@SiO_2-H_{14}[NaP_5W_{30}O_{110}]$  (Fig. 3c) the appeared peaks in the regions about  $3565$ ,  $1090$ ,  $960$ ,  $913$ ,  $794$  and  $566\text{ cm}^{-1}$  confirm the successful immobilization of the  $H_{14}[NaP_5W_{30}O_{110}]$  on the surface of  $NiFe_2O_4@SiO_2$ .



**Fig 3.** The FT-IR spectrum of (a)  $\text{NiFe}_2\text{O}_4@\text{SiO}_2$  (NFS), (b) Preyssler ( $\text{H}_{14}[\text{NaP}_5\text{W}_{30}\text{O}_{110}]$ ) and (c)  $\text{NiFe}_2\text{O}_4@\text{SiO}_2\text{-H}_{14}[\text{NaP}_5\text{W}_{30}\text{O}_{110}]$  (NFS-PRS).

Fig 4a, b shows transmission electron microscopy (TEM) images of the synthesized  $\text{NiFe}_2\text{O}_4@\text{SiO}_2$  (NFS) and  $\text{NiFe}_2\text{O}_4@\text{SiO}_2\text{-H}_{14}[\text{NaP}_5\text{W}_{30}\text{O}_{110}]$  (NFS-PRS) respectively. In the TEM image of NFS-PRS (Fig. 4b), the darker parts prove good immobilizing of  $\text{H}_{14}[\text{NaP}_5\text{W}_{30}\text{O}_{110}]$  on the  $\text{NiFe}_2\text{O}_4@\text{SiO}_2$ . Also, the particle size dispersion diagram (Fig. 4c) from the  $\text{NiFe}_2\text{O}_4@\text{SiO}_2$  shows that these magnetic nanoparticles have a size between 25 to 97

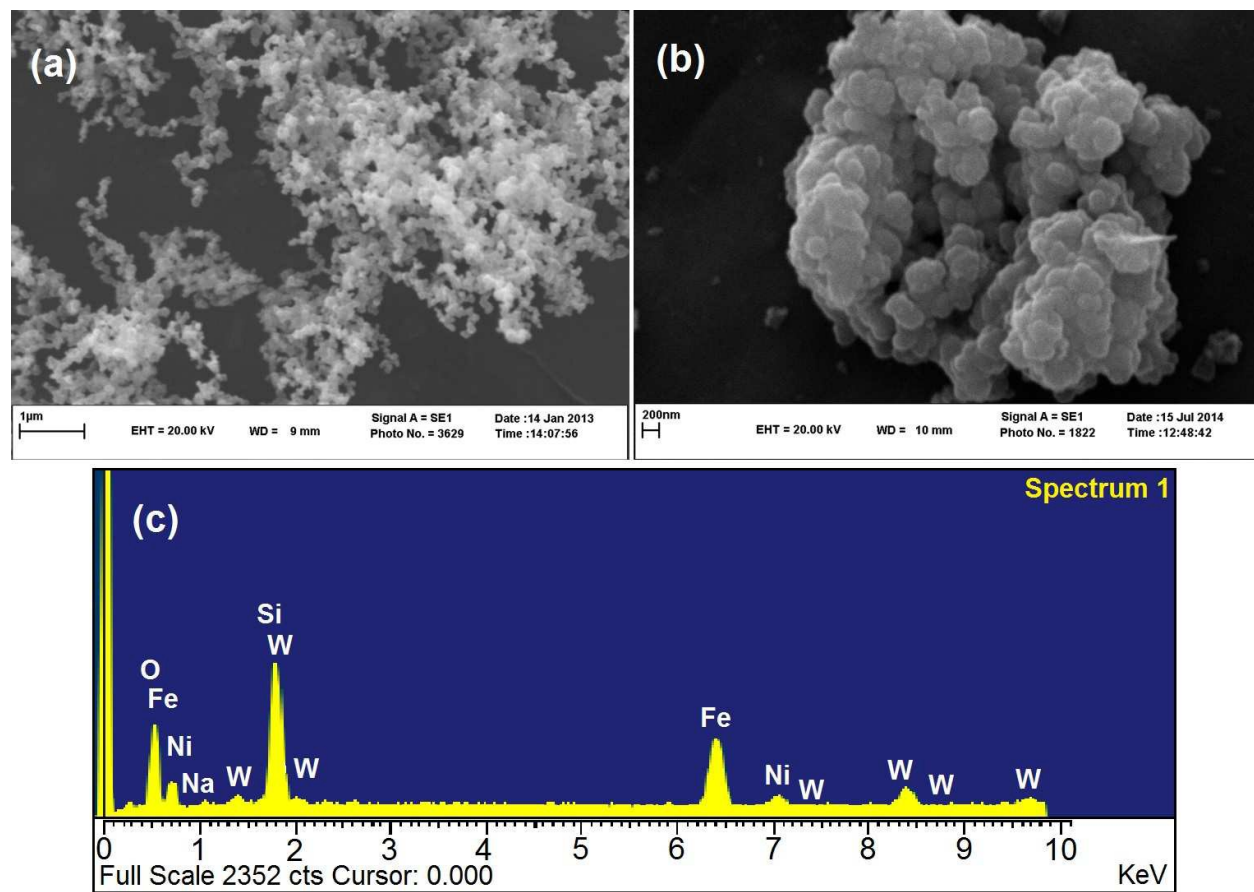
nm and mean diameter is 53 nm. Furthermore, the morphological features were studied by SEM technique.



**Fig 4.** TEM images of NiFe<sub>2</sub>O<sub>4</sub>@SiO<sub>2</sub> (NFS), and NiFe<sub>2</sub>O<sub>4</sub>@SiO<sub>2</sub>-H<sub>14</sub>[NaP<sub>5</sub>W<sub>30</sub>O<sub>110</sub>] (NFS-PRS) (a and b) and particle size dispersion of NiFe<sub>2</sub>O<sub>4</sub>@SiO<sub>2</sub> (NFS) (c).

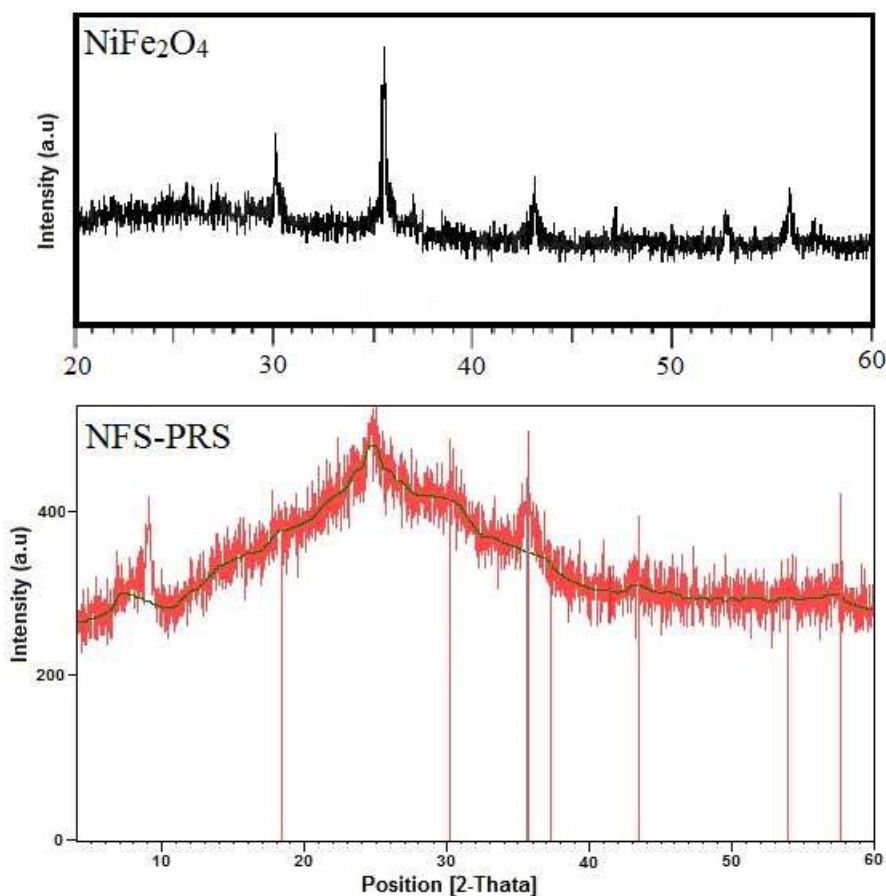
The SEM images before (Fig. 5a) and after (Fig. 5b) supported H<sub>14</sub>[NaP<sub>5</sub>W<sub>30</sub>O<sub>110</sub>] on the NiFe<sub>2</sub>O<sub>4</sub>@SiO<sub>2</sub> (NFS) demonstrate that these magnetic nanoparticles are almost spherical with

regular in shape. However, aggregation of nano particles was found and this aggregation might occur during the coating and supporting process. Moreover, in the energy dispersive X-ray spectrum (EDX) of  $\text{NiFe}_2\text{O}_4@\text{SiO}_2\text{-H}_{14}[\text{NaP}_5\text{W}_{30}\text{O}_{110}]$  (NFS-PRS) (Fig. 5c), the tungsten peaks confirm the successful immobilization of the  $\text{H}_{14}[\text{NaP}_5\text{W}_{30}\text{O}_{110}]$  on the surface of  $\text{NiFe}_2\text{O}_4@\text{SiO}_2$ . These observations are in agreement with FT-IR results.



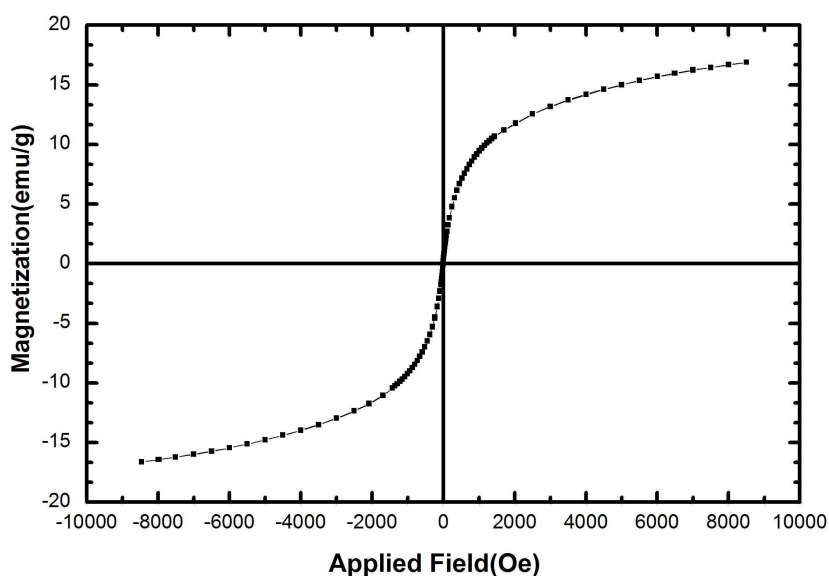
**Fig 5.** SEM images of  $\text{NiFe}_2\text{O}_4@\text{SiO}_2$  (NFS), and  $\text{NiFe}_2\text{O}_4@\text{SiO}_2\text{-H}_{14}[\text{NaP}_5\text{W}_{30}\text{O}_{110}]$  (NFS-PRS) (a and b) and EDX spectrum of  $\text{NiFe}_2\text{O}_4@\text{SiO}_2\text{-H}_{14}[\text{NaP}_5\text{W}_{30}\text{O}_{110}]$  (NFS-PRS) (c).

In XRD pattern of  $\text{NiFe}_2\text{O}_4$  (Fig. 6), the characteristic peaks at  $2\theta = 30, 35, 43, 54, 57$  and  $63$  are similar to the previously reported data for nonmagnetic particles  $\text{NiFe}_2\text{O}_4$ <sup>64-65</sup> and in XRD pattern of  $\text{NiFe}_2\text{O}_4@\text{SiO}_2\text{-H}_{14}[\text{NaP}_5\text{W}_{30}\text{O}_{110}]$  (NFS-PRS), the appeared broad peak at  $2\theta = 20\text{--}30$ , could be assigned an amorphous silica phase in the shell of  $\text{NiFe}_2\text{O}_4$ . However, there are no characteristic peaks of  $\text{H}_{14}[\text{NaP}_5\text{W}_{30}\text{O}_{110}]$  in this XRD pattern.<sup>62</sup> These observations indicate which  $\text{H}_{14}[\text{NaP}_5\text{W}_{30}\text{O}_{110}]$  is well-dispersed on the surface of  $\text{NiFe}_2\text{O}_4@\text{SiO}_2$  and there is no crystalline phase of this  $\text{H}_{14}[\text{NaP}_5\text{W}_{30}\text{O}_{110}]$  to be detected by XRD analysis.



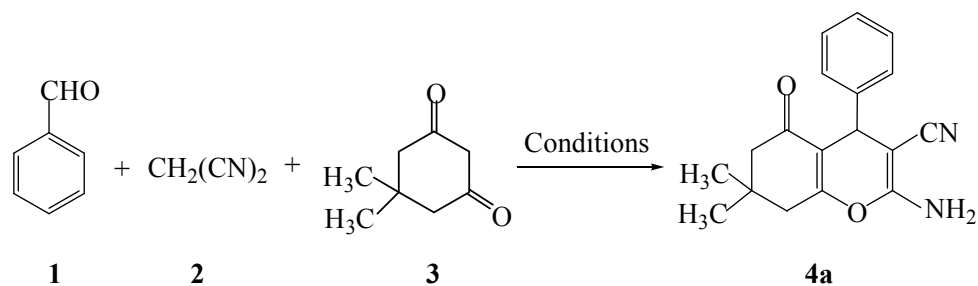
**Fig 6.** XRD pattern of  $\text{NiFe}_2\text{O}_4$  and  $\text{NiFe}_2\text{O}_4@\text{SiO}_2\text{-H}_{14}[\text{NaP}_5\text{W}_{30}\text{O}_{110}]$  (NFS-PRS)

It is important that the core/shell material should possess sufficient magnetic and superparamagnetic properties for its practical applications. Magnetic hysteresis measurements for the  $\text{NiFe}_2\text{O}_4$  were done in an applied magnetic field at r.t, with the field sweeping from  $-10000$  to  $+10000$  Oersted. As shown in Fig. 7, the  $M(H)$  hysteresis loop for the samples was completely reversible, showing that the nanoparticles exhibit superparamagnetic characteristics. The hysteresis loops of them reached saturation up to the maximum applied magnetic field. The magnetic saturation values of the  $\text{NiFe}_2\text{O}_4$  are  $16.71 \text{ emu g}^{-1}$  at r.t. These nonmagnetic particles showed high permeability in magnetization and their magnetization was sufficient for magnetic separation with a conventional magnet.



**Fig 7.** VSM curve of  $\text{NiFe}_2\text{O}_4$  at room temperature.

To achieve the optimization reaction conditions, at first, a mixture benzaldehyde (1 mmol), malononitrile **2** (2 mmol) and dimedone **3** (1 mmol), as model reaction, was stirred in ethanol (2 ml) in the presence of different amounts of NiFe<sub>2</sub>O<sub>4</sub>@SiO<sub>2</sub>-H<sub>14</sub>[NaP<sub>5</sub>W<sub>30</sub>O<sub>110</sub>] (NFS-PRS) under reflux conditions (*Table 1, entries 1-3*). We also tested this obtained condition (0.02 g of NFS-PRS) in the present of different solvents (2 ml, entries 4-6). As it is shown as Table 1, indicates that ethanol is more suitable solvent in the synthesis of **4a**. When the reaction was performed under solvent-free conditions, a low yield of target product was obtained (*Entry 7*). To improve the yield and decrease the reaction time, the ultrasonic conditions was examined using NiFe<sub>2</sub>O<sub>4</sub>@SiO<sub>2</sub>-H<sub>14</sub>[NaP<sub>5</sub>W<sub>30</sub>O<sub>110</sub>] NFS-PRS (0.02 g) in ethanol at room temperature (entry 8). To further improve the yield and decrease the reaction time, we tried to increase the reaction temperature under ultrasound irradiation (entries 9-10). It can be seen from the Table 1 that there was no remarkable temperature effect on this reaction. The use of NiFe<sub>2</sub>O<sub>4</sub> (NFS), and H<sub>14</sub>[NaP<sub>5</sub>W<sub>30</sub>O<sub>110</sub>] as the catalysts in this reaction resulted in low yields of the product after longer reaction times (entries 11–12). In an effort to evaluate the catalytic activity, several other heteropoly, inorganic and organic acids were examined in this reaction and the results are summarized in Table 1. As can be seen from this table, among the catalysts screened, NiFe<sub>2</sub>O<sub>4</sub>@SiO<sub>2</sub>-H<sub>14</sub>[NaP<sub>5</sub>W<sub>30</sub>O<sub>110</sub>] (NFS-PRS) with 0.02 g catalyst loading proved to be superior to others in producing the best yield (92 %) at room temperature under ultrasound-irradiation condition (entry 8). When the reaction was attempted without a catalyst, it was found that only a trace amount of product was obtained (entries 16-17).

**Table 1.** Optimization of Reaction Conditions

Entry	Catalyst (g)	Conditions	Time (min)	Yield <sup>a</sup> (%)
1	NFS-PRS (0.02 g)	Ethanol/reflux	20	74
2	NFS-PRS (0.03 g)	Ethanol/reflux	20	65
3	NFS-PRS (0.01 g)	Ethanol/reflux	20	56
4	NFS-PRS (0.02 g)	Water/reflux	20	54
5	NFS-PRS (0.02 g)	Methanol/reflux	20	70
6	NFS-PRS (0.02 g)	Acetonitrile/reflux	20	32
7	NFS-PRS (0.02 g)	Solvent-free/80 <sup>0</sup> C	20	53
8	NFS-PRS (0.02 g)	Ethanol/US/rt	5	92
9	NFS-PRS (0.02 g)	Ethanol/US/35 <sup>0</sup> C	5	90
10	NFS-PRS (0.02 g)	Ethanol/US/45 <sup>0</sup> C	5	86
11	NFS (0.02 g)	Ethanol/US/rt	10	28
12	PRS (0.02 g)	Ethanol/US/rt	10	59
13	H <sub>2</sub> SO <sub>4</sub> (3 drops)	Ethanol/US/rt	10	30
14	Oxalic acid (0.02 g)	Ethanol/US/rt	10	48

15	CH <sub>3</sub> COOH (0.1 ml)	Ethanol/US/rt	10	24
16	-- <sup>b</sup>	Ethanol/reflux	60	trace
17	-- <sup>b</sup>	Ethanol/US/rt	60	trace

<sup>a</sup>Isolated yield. <sup>b</sup>This reaction was carried out in the absence of NFS-PRS.

The reaction was successful both with and without ultrasound in ethanol, but, the use of ultrasound afforded higher yields. Ethanol irradiated with ultrasound can produce tiny bubbles that can undergo a violent collapse known as cavitation, which generates localized microscopic “hot spots” with transient high temperatures and pressures to induce favorable conditions for reactions. The reason for the choice of solvent is explained on the basis of the fact that solvent affects the transition state, and when polar substrates are used in the synthesis, the transition state is better solvated by polar solvent and the reaction rate increases, which increases the product yield. Also EtOH is the most suitable solvent for the even dispersion of catalyst.

Under the optimized reaction conditions (Table 1, entry 8), a range of tetrahydrobenzo[b]pyrans and 2-amino-3-cyano-4H-pyrans (**4a-o**, **6a-f**) were synthesized via the one-pot condensation of malononitrile, various aldehydes, and 1,3-dicarbonyl compounds (1,3-cyclohexanedione or 5,5-dimethyl-1,3-cyclohexanedione or ethyl acetoacetate) under ultrasonic irradiation (Table 3). In this reaction system, electron withdrawing substituents and lower steric hindrance gave higher yields than the derivatives contain electron-donating groups and higher steric hindrance.

Finally, we have developed this synthetic method for one-pot efficient synthesis of pyrano[2,3-*c*]pyrazoles (**8a-f**) by replacing 1,3-dicarbonyl compounds (1,3-cyclohexanedione or

5,5-dimethyl-1,3-cyclohexanedione or ethyl acetoacetate) with 3-methyl-1-phenyl-2-pyrazoline-5-one (**7**) under previous optimized condition. All reactions proceeded efficiently and the desired products (**8a-f**) were obtained from high to excellent yields in relatively short times without any formation of by-products (Table 3).

After successfully synthesizing of a series of pyrano[2,3-c]pyrazoles (**8a-f**) in good yields, we replaced 3-methyl-1-phenyl-2-pyrazoline-5-one (**7**) with hydrazine hydrate (**9**) and ethyl acetoacetate (**5**) in same conditions for synthesis of (**10a-g**) compounds in the presence of a catalytic amount of NiFe<sub>2</sub>O<sub>4</sub>@SiO<sub>2</sub>-H<sub>14</sub>[NaP<sub>5</sub>W<sub>30</sub>O<sub>110</sub>] (NFS-PRS). In order to optimize reaction conditions, the reaction of synthesis **10a** was chosen as a model reaction and the effect of different amount of catalyst, temperatures and solvents, was studied. It seems that 0.02 g of NFS-PRS under ultrasonic irradiation at room temperature has acted better than other conditions and EtOH showed better result as solvent (Table 2). Under these optimal conditions, the scope and specificity of this protocol was further investigated by application of various aldehydes (Table 3).

**Table 2.** Optimization of Reaction Conditions for synthesis of **10a**

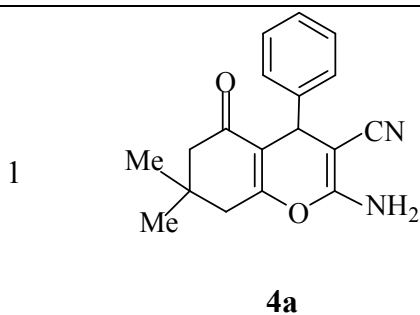
Entry	NFS-PRS (g)	Conditions	Time (min)	Yield <sup>a</sup> (%)
1	0.02	Ethanol/reflux	40	72

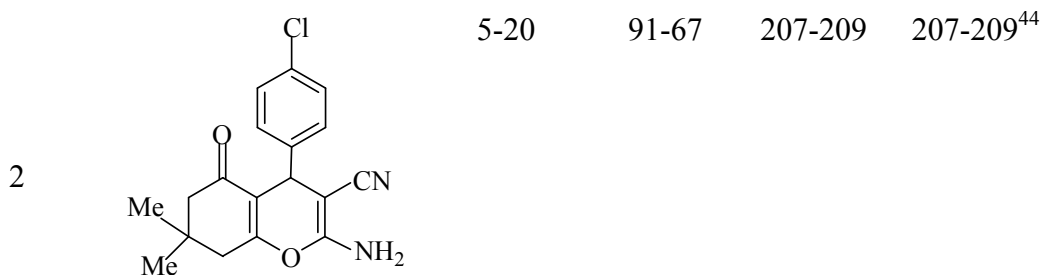
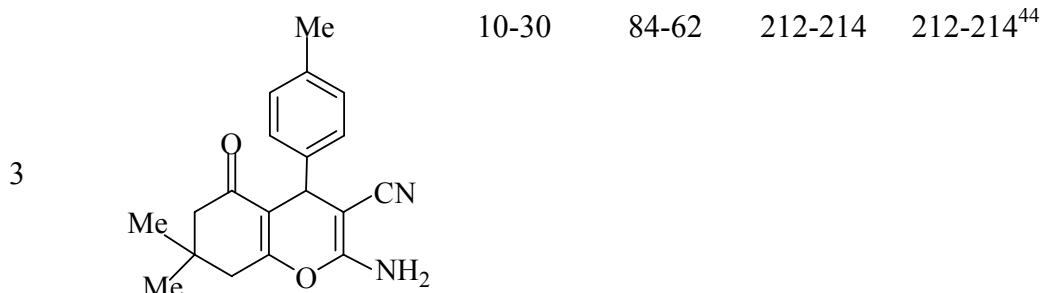
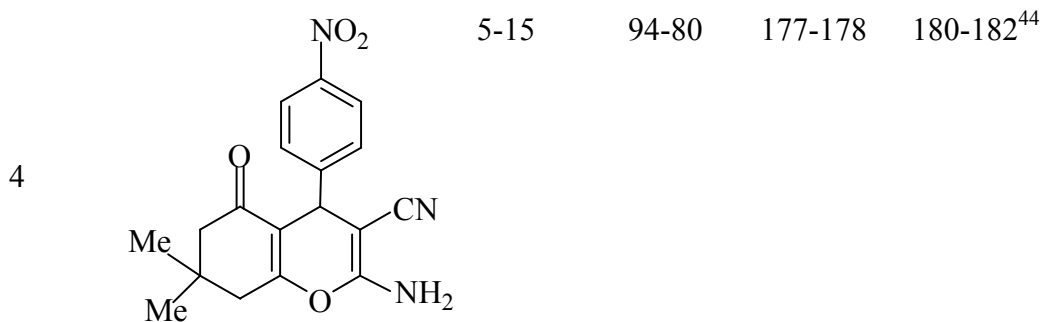
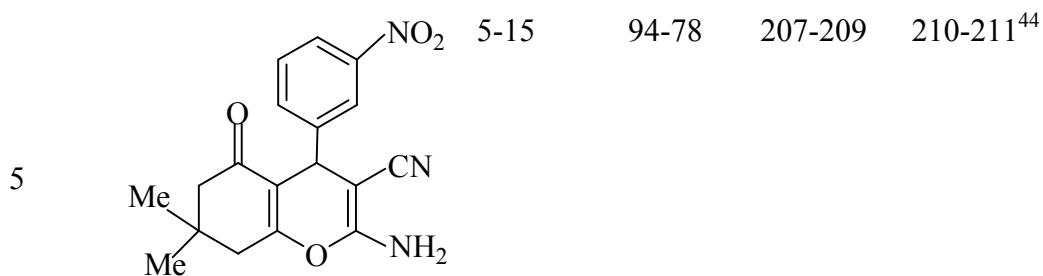
2	0.03	Ethanol/reflux	40	61
3	0.01	Ethanol/reflux	40	52
4	0.02	Water/reflux	40	50
5	0.02	Methanol/reflux	40	67
6	0.02	Acetonitrile/reflux	40	32
7	0.02	Ethanol/US/rt	10	90
8	0.02	Ethanol/US/35 <sup>0</sup> C	10	90

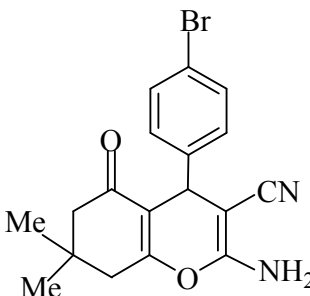
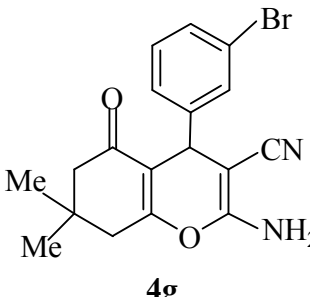
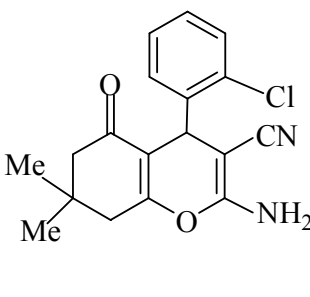
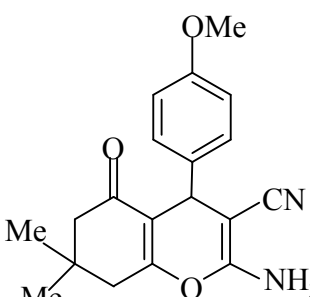
<sup>a</sup>Isolated yield.

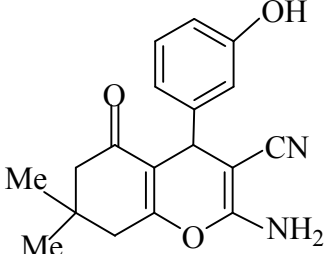
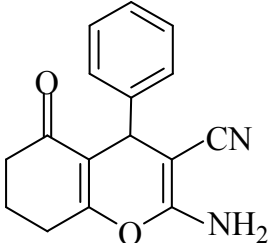
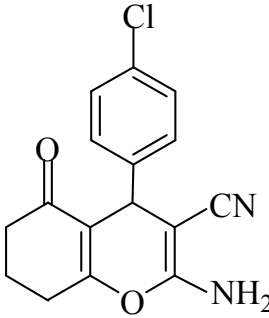
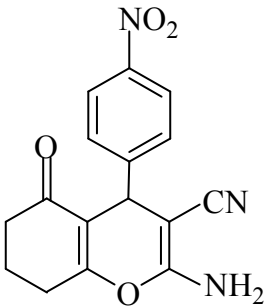
**Table 3.** One-pot and green synthesis of tetrahydrobenzo[b]pyrans, 2-amino-3-cyano-4H-pyrans, and pyrano [2, 3-c]pyrazoles under both conventional and ultrasonic waves conditions

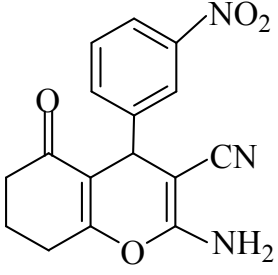
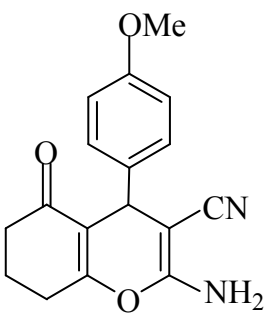
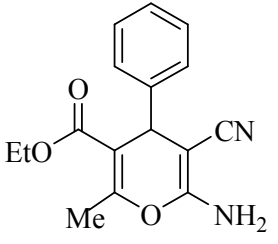
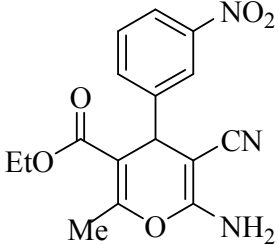
Entry	Products ( <b>4a-o</b> , <b>6a-f</b> , <b>8a-f</b> , <b>10a-g</b> )	Time <sup>a</sup> (min)	Yield <sup>b</sup> (%)	Mp ( <sup>0</sup> C)	
				Found	Lit.
		<b>I-II</b>	<b>I-II</b>		
		5-20	92-74	227-228	227-239 <sup>44</sup>

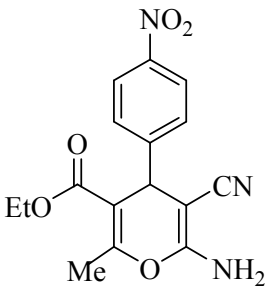
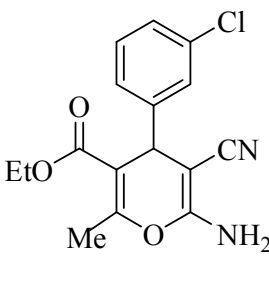
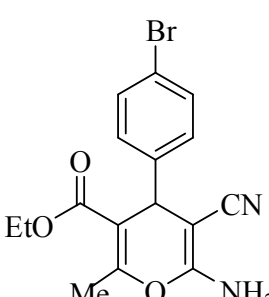
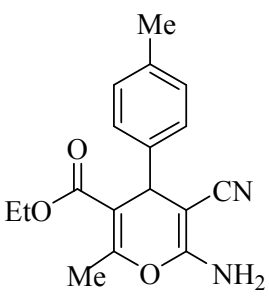


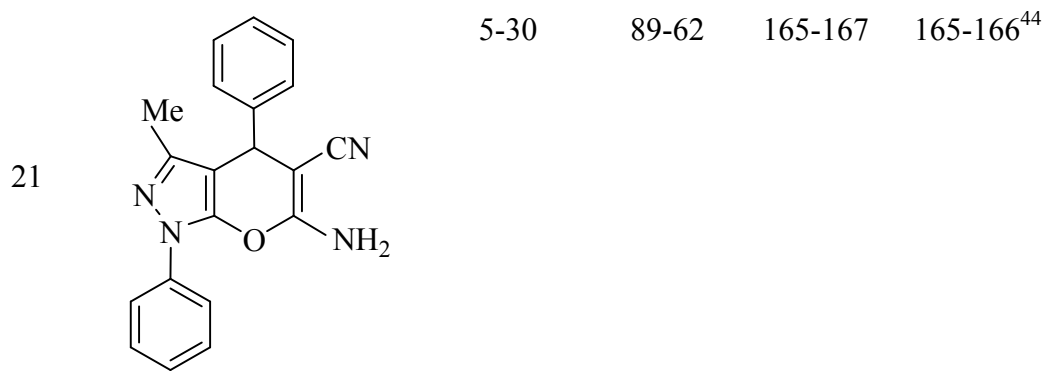
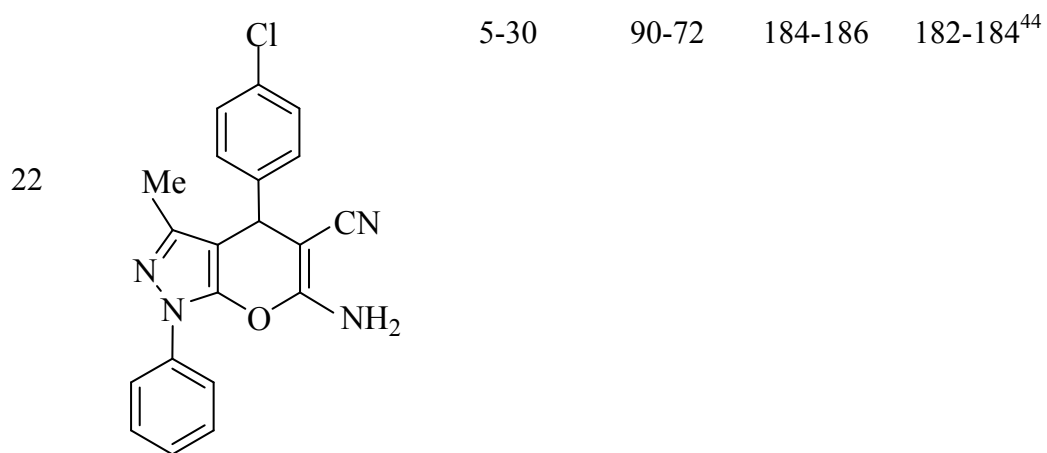
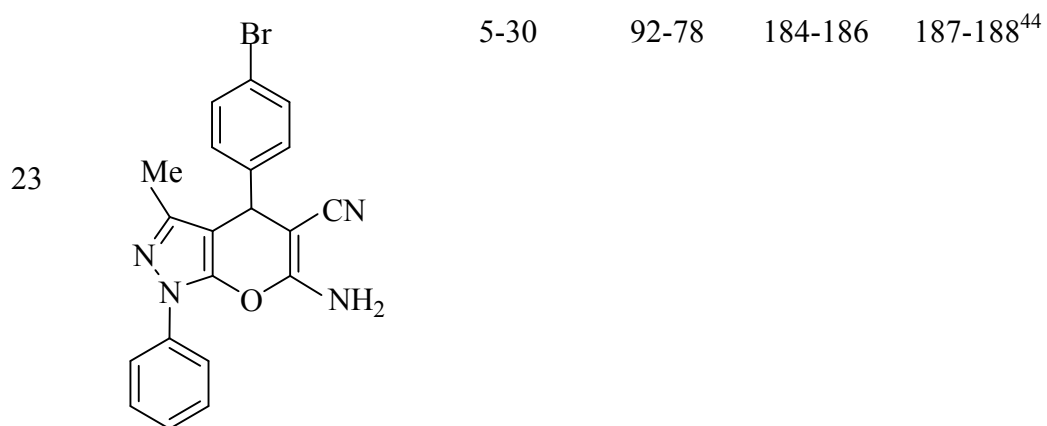
**4b****4c****4d****4e**

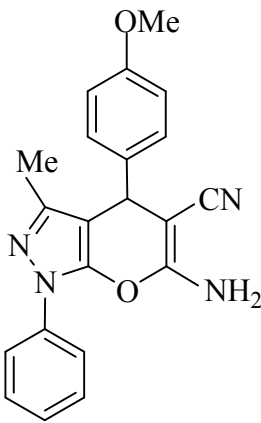
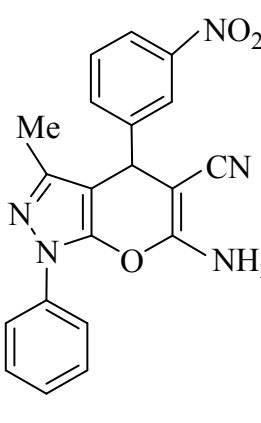
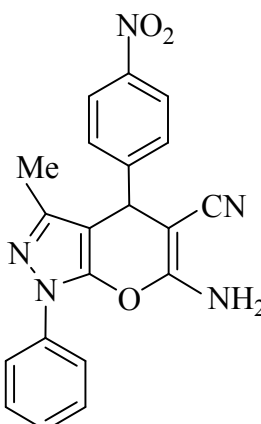
6	 <b>4f</b>	10-25	89-66	199-201	195-197 <sup>44</sup>
7	 <b>4g</b>	10-20	90-78	225-227	228-230 <sup>45</sup>
8	 <b>4h</b>	10-30	80-57	215-216	214-216 <sup>40</sup>
9	 <b>4i</b>	5-20	91-73	195-197	216-218 <sup>44</sup>

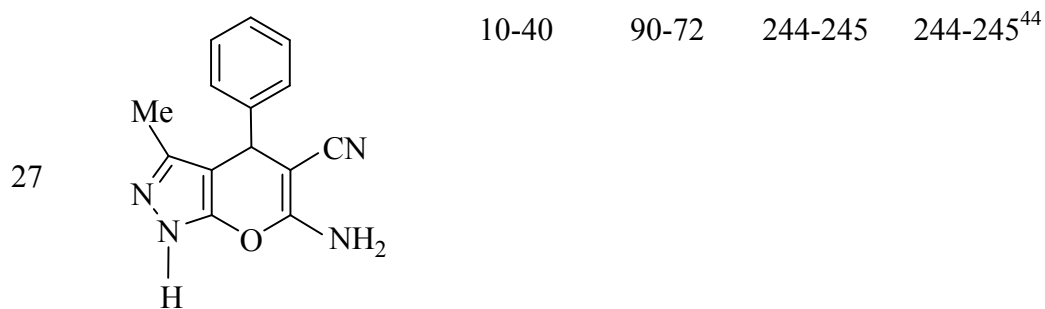
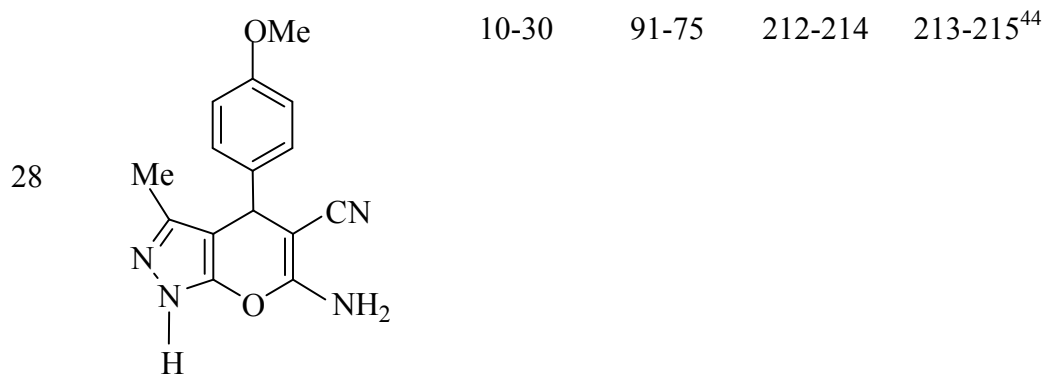
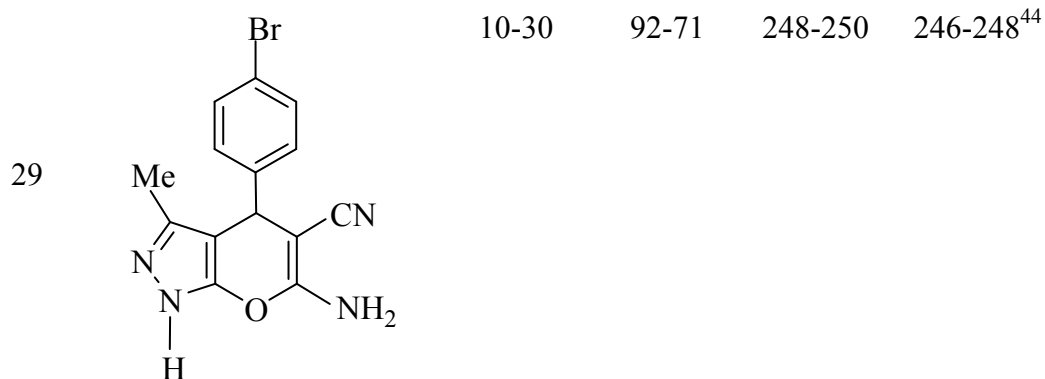
10		15-35	81-60	232-234	236-238 <sup>44</sup>
11		5-20	90-60	229-231	234-236 <sup>44</sup>
12		5-20	89-66	226-227	224-226 <sup>44</sup>
13		5-15	92-78	232-233	230-232 <sup>44</sup>

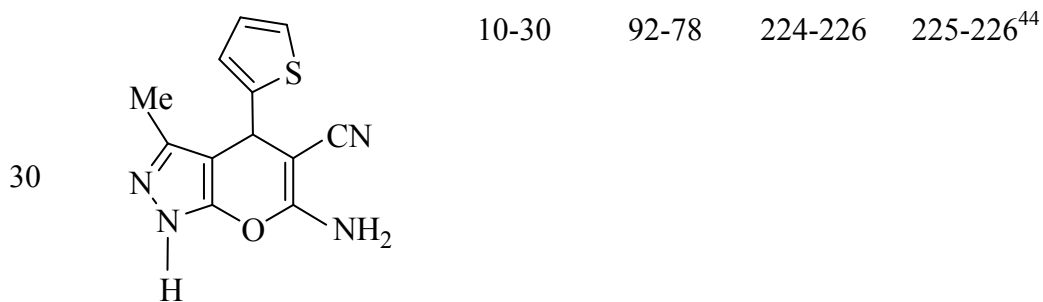
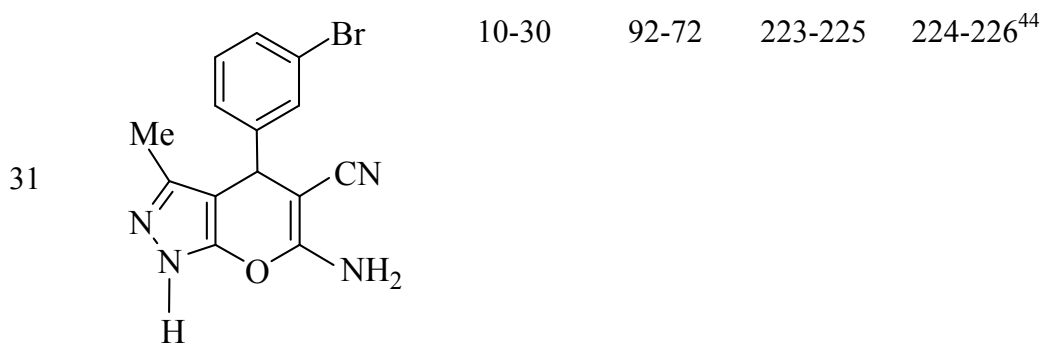
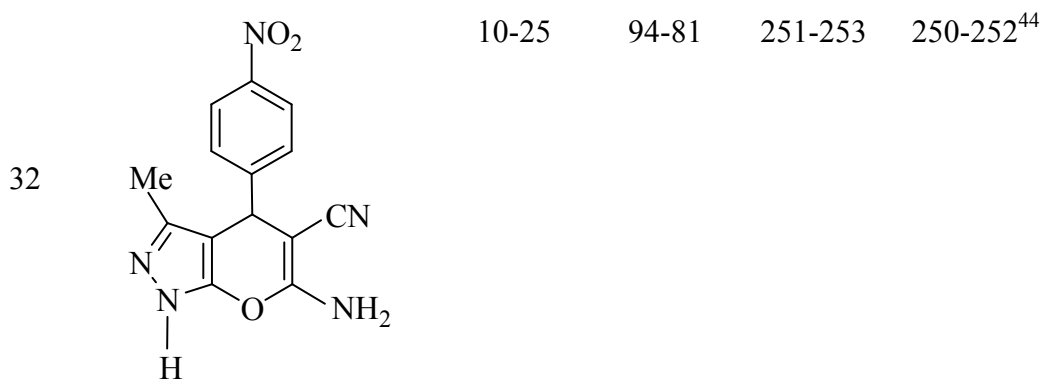
14		5-15	91-80	236-238	237-239 <sup>44</sup>
	<b>4n</b>				
15		10-30	90-70	189-190	190-192 <sup>38</sup>
	<b>4o</b>				
15		20-300	86-60	189-191	190-192 <sup>44</sup>
	<b>6a</b>				
16		15-180	92-72	184-187	187-188 <sup>52</sup>
	<b>6b</b>				

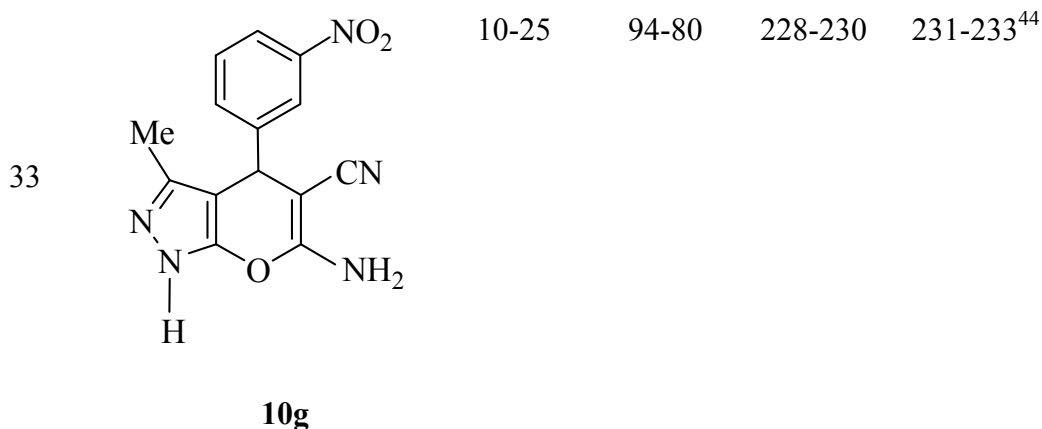
17	 <b>6c</b>	15-180	91-74	174-176	175-175 <sup>52</sup>
18	 <b>6d</b>	20-240	87-66	177-179	180-181 <sup>52</sup>
19	 <b>6e</b>	20-240	86-64	182-184	180-181 <sup>52</sup>
20	 <b>6f</b>	35-360	83-56	175-176	175-176 <sup>52</sup>

**8a****8b****8c**

24		5-30	90-74	172-173	170-172 <sup>44</sup>
	<b>8d</b>				
25		5-20	94-80	189-190	190-192 <sup>44</sup>
	<b>8e</b>				
26		5-20	93-82	196-197	197-199
	<b>8f</b>				

**10a****10b****10c**

**10d****10e****10f**



<sup>a</sup>Reaction under ultrasonic irradiation at room temperature and the ultrasonic power 250 W, irradiation frequency 40 kHz (**I**), under reflux conditions in ethanol (**II**). <sup>b</sup>Isolated yields.

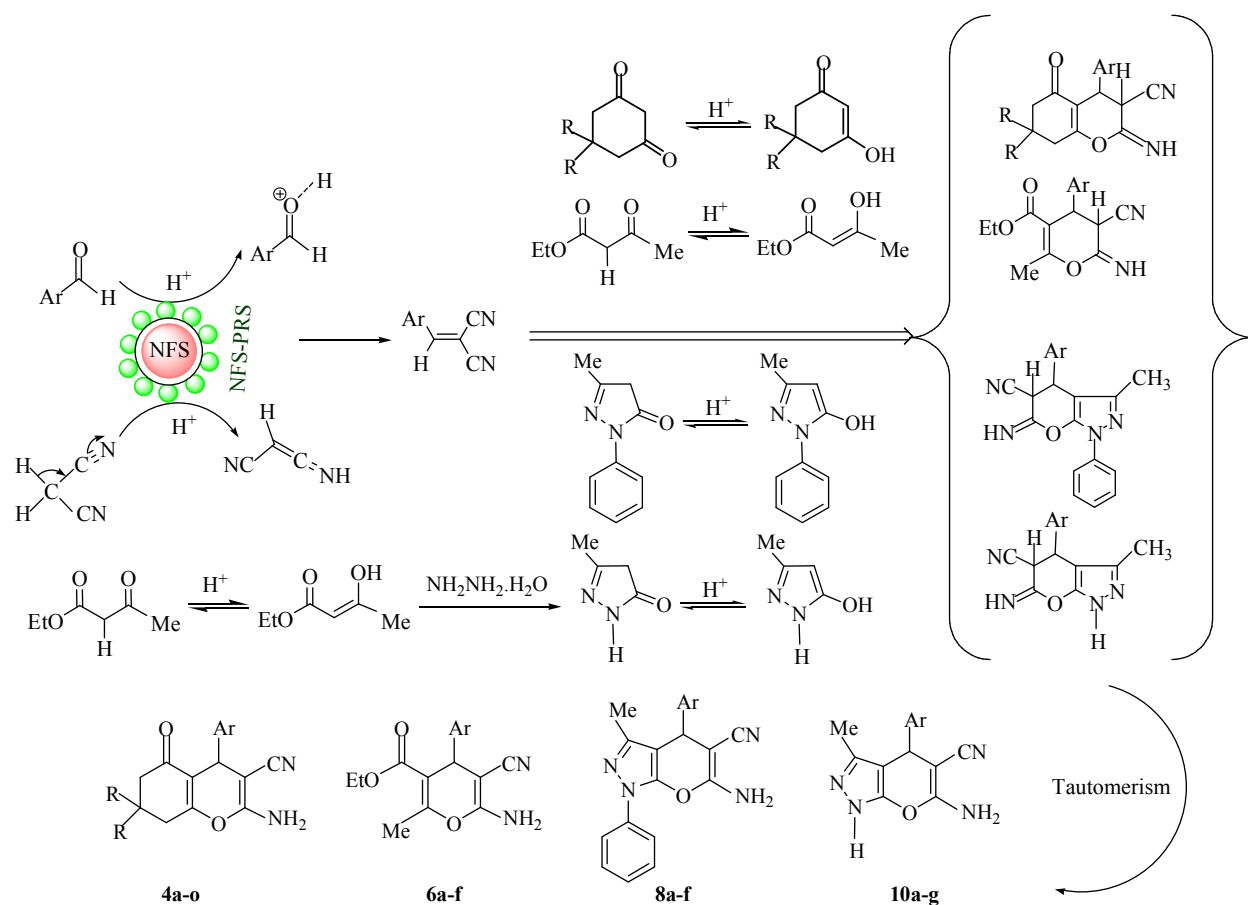
In all reactions mentioned above, the reaction procedure was simple, clean and completion of the reaction was identified by TLC. Generally the product formed after completion of the reaction is separated from catalyst by tedious work up procedures which are not energy efficient and green. Further the purification of products by traditional methods (column chromatography) does not support green chemistry principles as large amount of organic solvent was used. But in our protocol the catalyst was separated from reaction product using external magnet within seconds.

The recovery and reusability of catalyst is an important aspect for chemists from economic, cost effectiveness and environmental point of view. For this purpose, the recycling of NFS-PRS was investigated using the synthesis of **4a** and **8c**. After the completion of the reaction, the NFS-PRS catalyst was separated from the reaction mixture by use of an external magnetic field, dried at 100 °C for 2 h, and re-used in the same reaction. It was re-used in the model reactions to give

**4a** and **8c** in yields of 92%, 92%, 90%, 89% and 92%, 90%, 90%, 88% respectively, for four consecutive runs.

Environmentally friendly is becoming increasingly important in modern organic synthesis. This requires us to avoid the use of toxic solvents and reagents, minimize the energy requirement, and utilize renewable catalysts. The use of ultrasonic irradiation and  $\text{NiFe}_2\text{O}_4@\text{SiO}_2\text{-H}_{14}[\text{NaP}_5\text{W}_{30}\text{O}_{110}]$  are items that can fulfill these requirements.  $\text{NiFe}_2\text{O}_4@\text{SiO}_2\text{-H}_{14}[\text{NaP}_5\text{W}_{30}\text{O}_{110}]$  is easily separated using a magnet and can be re-used without loss of activity. It is very stable due to moisture insensitivity, highly efficient due to its greater surface area and inexpensive because of the re-usability. These properties make  $\text{NiFe}_2\text{O}_4@\text{SiO}_2\text{-H}_{14}[\text{NaP}_5\text{W}_{30}\text{O}_{110}]$  attractive as novel magnetically separable catalyst for the synthesis of highly substituted pyran derivatives. Also, the ultrasound can be raised the rate of reaction and therefore reduced the energy consumption.

We herein propose a mechanism in Scheme 2 for the formation of highly substituted pyran derivatives under the reaction conditions where  $\text{NiFe}_2\text{O}_4@\text{SiO}_2\text{-H}_{14}[\text{NaP}_5\text{W}_{30}\text{O}_{110}]$  (NFS-PRS) catalyst acts as an acid.



**Scheme 2.** Proposed mechanism for the synthesis of highly substituted pyran derivatives

In order to examine the efficiency of the present method for the synthesis of highly substituted pyran derivatives, compounds **4a**, **4e**, **4l**, **8c** and **10c** were compared with some of those reported in the literature (Table 4). As can be seen, the reaction catalyzed by NiFe<sub>2</sub>O<sub>4</sub>@SiO<sub>2</sub>-H<sub>14</sub>[NaP<sub>5</sub>W<sub>30</sub>O<sub>110</sub>] gives a comparable yield and requires less time than other protocols. Even other functionalized magnetic nano particles does not show better results than our catalyst.

**Table 4.** Comparison of present method with other reported protocols for the synthesis of highly substituted pyran derivatives

Product	Reaction conditions	Time (min)	Yield (%) <sup>a</sup>	Ref
<b>4a</b>	Fe <sub>3</sub> O <sub>4</sub> @SiO <sub>2</sub> -imid-PMA/H <sub>2</sub> O/Us/rt	7	96	[36]
	Tetra-methyl ammonium hydroxide/H <sub>2</sub> O/rt	120	81	[37]
	NH <sub>4</sub> H <sub>2</sub> PO <sub>4</sub> /Al <sub>2</sub> O <sub>3</sub> /EtOH/Reflux	15	86	[40]
	Fe <sub>3</sub> O <sub>4</sub> @SiO <sub>2</sub> @NH-NH <sub>2</sub> -PW/H <sub>2</sub> O/Reflux	40	90	[41]
	Magnetic La <sub>0.7</sub> Sr <sub>0.3</sub> MnO <sub>3</sub> nanoparticles/EtOH/Us/rt	12	92	[42]
	Fe <sub>3</sub> O <sub>4</sub> @SiO <sub>2</sub> @TiO <sub>2</sub> /Solvent-free/100 <sup>0</sup> C	20	93	[45]
	Urea/EtOH: H <sub>2</sub> O (1:1, v:v)/rt	120	90	[55]
	NiFe <sub>2</sub> O <sub>4</sub> @SiO <sub>2</sub> @H <sub>14</sub> [NaP <sub>5</sub> W <sub>30</sub> O <sub>110</sub> ]/EtOH/Us/rt	5	92	Present work
<b>4e</b>	Fe <sub>3</sub> O <sub>4</sub> @SiO <sub>2</sub> -imid-PMA/H <sub>2</sub> O/Us/rt	7	95	[36]
	Tetra-methyl ammonium hydroxide/H <sub>2</sub> O/rt	120	92	[37]
	Potassium phosphate/EtOH: H <sub>2</sub> O (80:20, v:v)/rt	45	89	[38]
	NH <sub>4</sub> H <sub>2</sub> PO <sub>4</sub> /Al <sub>2</sub> O <sub>3</sub> /EtOH/Reflux	15	90	[40]
	Magnetic La <sub>0.7</sub> Sr <sub>0.3</sub> MnO <sub>3</sub> nanoparticles/EtOH/Us/rt	8	98	[42]
	Nano Na <sub>2</sub> CaP <sub>2</sub> O <sub>7</sub> /H <sub>2</sub> O/Reflux	10	94	[50]
	NiFe <sub>2</sub> O <sub>4</sub> @SiO <sub>2</sub> @H <sub>14</sub> [NaP <sub>5</sub> W <sub>30</sub> O <sub>110</sub> ]/EtOH/Us/rt	5	94	Present work
<b>4l</b>	Potassium phosphate/EtOH: H <sub>2</sub> O (80:20)/rt	60	89	[38]
	NH <sub>4</sub> H <sub>2</sub> PO <sub>4</sub> /Al <sub>2</sub> O <sub>3</sub> /EtOH/Reflux	25	84	[40]
	NiFe <sub>2</sub> O <sub>4</sub> @SiO <sub>2</sub> -H <sub>3</sub> PW <sub>12</sub> O <sub>40</sub> /EtOH/Reflux	25	82	[44]
	NiFe <sub>2</sub> O <sub>4</sub> @SiO <sub>2</sub> @H <sub>14</sub> [NaP <sub>5</sub> W <sub>30</sub> O <sub>110</sub> ]/EtOH/Us/rt	5	89	Present work
<b>8c</b>	NH <sub>4</sub> H <sub>2</sub> PO <sub>4</sub> /Al <sub>2</sub> O <sub>3</sub> /Solvent-free/80 <sup>0</sup> C	20	85	[40]
	Magnetic La <sub>0.7</sub> Sr <sub>0.3</sub> MnO <sub>3</sub> nanoparticles/EtOH/Us/rt	11	87	[42]
	NiFe <sub>2</sub> O <sub>4</sub> @SiO <sub>2</sub> -H <sub>3</sub> PW <sub>12</sub> O <sub>40</sub> /EtOH/Reflux	5	90	[44]
	Nano Na <sub>2</sub> CaP <sub>2</sub> O <sub>7</sub> /H <sub>2</sub> O/Reflux	15	90	[50]
	NiFe <sub>2</sub> O <sub>4</sub> @SiO <sub>2</sub> @H <sub>14</sub> [NaP <sub>5</sub> W <sub>30</sub> O <sub>110</sub> ]/EtOH/Us/rt	5	92	Present work

	NH <sub>4</sub> H <sub>2</sub> PO <sub>4</sub> /Al <sub>2</sub> O <sub>3</sub> /EtOH/Reflux	80	78	[40]
<b>10c</b>	NiFe <sub>2</sub> O <sub>4</sub> @SiO <sub>2</sub> -H <sub>3</sub> PW <sub>12</sub> O <sub>40</sub> /EtOH/Reflux	45	90	[44]
	Nano Na <sub>2</sub> CaP <sub>2</sub> O <sub>7</sub> /H <sub>2</sub> O/Reflux	15	85	[50]
	NiFe <sub>2</sub> O <sub>4</sub> @SiO <sub>2</sub> @H <sub>14</sub> [NaP <sub>5</sub> W <sub>30</sub> O <sub>110</sub> ]/EtOH/Us/rt	10	92	Present work

<sup>a</sup> Isolated yields.

## Conclusion

In conclusion, a simple ultrasonic procedure was evaluated for the synthesis of highly substituted pyrans (tetrahydrobenzo[b]pyrans, 2-amino-3-cyano-4H-pyran, and pyrano [2, 3-c]pyrazoles) using silica-coated magnetic NiFe<sub>2</sub>O<sub>4</sub> nanoparticles-supported H<sub>14</sub>[NaP<sub>5</sub>W<sub>30</sub>O<sub>110</sub>] (NFS-PRS) as an efficient, green and reusable catalyst. The characteristics features of the catalyst includes its simple and facile preparation, cost effectiveness, easy and rapid separation from reaction product, reusability and eco-friendly nature which make it superior, excellent and sustainable catalytic system in comparison with other catalyst. All the key features of present protocol such as simplicity, efficiency, high yield, shorter reaction time, no need of traditional separation and purification method are agreement with green chemistry profile. Also, we have presented that the ultrasound can be raised the rate of reaction and therefore reduced the energy consumption.

## Experimental Section

All reagents were obtained from commercial sources and were used without purification. The FT-IR spectra were recorded on a Shimadzu 435-U-04 spectrophotometer (KBr pellets). <sup>1</sup>H NMR spectra were obtained using Bruker 250 and 300 MHz spectrometers in DMSO-d<sub>6</sub> or

$\text{CDCl}_3$  and using TMS as the internal reference. Melting points were determined in open capillary tubes in a Stuart BI Branstead Electrothermal cat no. IA9200 apparatus and uncorrected. The particle size and morphology of the synthesized catalyst were characterized with a transmission electron microscope (TEM) (Philips CM-200 and Titan Krios) and scanning electron microscope (SEM) (Philips XL 30 and S-4160) with gold coating. The size dispersion of the samples was obtained using a laser particle size analyzer (CORDOUAN, Vasco3).

### **General Procedure for the Synthesis of silica-coated magnetic $\text{NiFe}_2\text{O}_4$ nanoparticles-supported $\text{H}_{14}[\text{NaP}_5\text{W}_{30}\text{O}_{110}]$ (NFS-PRS)**

Nano- $\text{NiFe}_2\text{O}_4@\text{SiO}_2$  (1 g) was dispersed in water (50 mL) sonicated for 15 min at room temperature.  $\text{H}_{14}[\text{NaP}_5\text{W}_{30}\text{O}_{110}]$  (0.75 g) dissolved in water (5 mL) was added drop wise to this solution and then the mixture was stirred for 12 h at room temperature under vacuum. After stirring the mentioned time, the solvent was evaporated and the supported catalyst collected by a permanent magnet and dried in a vacuum overnight and after first drying, the supported nano catalyst was calcined at 250 °C temperature for 2 h.

### **General Procedure for the Synthesis of Tetrahydrobenzo[b]pyrans (4a-o), 2-Amino-3-cyano-4H-pyrans (6a-f), and Pyrano[2,3-c]pyrazoles (8a-f) under thermal conditions**

The catalyst, NFS-PRS (0.02 g), was added to a mixture of the aldehydes **1** (1 mmol), malononitrile **2** (0.08 g, 1.2 mmol), and dimedone or 1,3-cyclohexandione **3** or ethyl acetoacetate **5** or 3-methyl-1-phenyl-2-pyrazoline-5-one **7** (1 mmol), and 5 ml of ethanol in a 20 ml round bottom flask fitted with a reflux condenser. The resulting mixture was heated to reflux (an oil bath) for the appropriate time (*see Table 2*) with stirring (spin bar). After the completion of the reaction as determined by TLC (hexane-ethyl acetate, 4:1), the nanomagnetic catalyst was

separated from the reaction mixture by use of an external magnetic field. The resulting crude product was poured into crushed ice, and the solid product which separated was isolated by filtration and recrystallized from ethanol (5 ml) to afford tetrahydrobenzo[b]pyrans (**4a-o**), 2-amino-3-cyano-4H-pyrans (**6a-f**), and pyrano[2,3-c]pyrazoles (**8a-f**).

#### **General Procedure for the Synthesis of Tetrahydrobenzo[b]pyrans (4a-o), 2-Amino-3-cyano-4H-pyrans (6a-f), and Pyrano[2,3-c]pyrazoles (8a-f) under ultrasound irradiation**

The catalyst, NFS-PRS (0.02 g), was added to a mixture of the aldehydes **1** (1 mmol), malononitrile **2** (0.08 g, 1.2 mmol), and dimedone or 1,3-cyclohexandione **3** or ethyl acetoacetate **5** or 3-methyl-1-phenyl-2-pyrazoline-5-one **7** (1 mmol), and 5 ml of ethanol in a 20 ml round bottom flask. The reaction mixture was irradiated under sonication at room temperature for appropriate time as shown in Table 2. To maintain the ultrasonic bath temperature, cold/hot water was either added or removed manually. After the completion of the reaction as determined by TLC (hexane-ethyl acetate, 4:1), the nanomagnetic catalyst was separated from the reaction mixture by use of an external magnetic field. The resulting crude product was poured into crushed ice, and the solid product which separated was isolated by filtration and recrystallized from ethanol (5 ml) to afford tetrahydrobenzo[b]pyrans (**6a-o**), 2-amino-3-cyano-4H-pyrans (**6a-f**), and pyrano[2,3-c]pyrazoles (**8a-f**).

#### **General Procedure for four component synthesis of Pyrano[2,3-c]pyrazoles (10a-g) under thermal and ultrasound irradiation conditions**

The catalyst, NFS-PRS (0.02 g), was added to a mixture of the aldehydes **1** (1 mmol), malononitrile **2** (0.08 g, 1.2 mmol), hydrazine hydrate **9** (1.2 mmol) and ethyl acetoacetate **5** (1 mmol), and 5 ml of ethanol in a 20 ml round bottom flask fitted with a reflux condenser. The

resulting mixture was heated to reflux (an oil bath) for the appropriate time (*see Table 2*) with stirring (spin bar). After the completion of the reaction as determined by TLC (hexane-ethyl acetate, 4:1), the nanomagnetic catalyst was separated from the reaction mixture by use of an external magnetic field. The resulting crude product was poured into crushed ice, and the solid product which separated was isolated by filtration and recrystallized from ethanol (5 ml) to afford pyrano[2,3-*c*]pyrazoles (**10a-g**). In a separate reaction, this condition exactly repeats under sonication at room temperature for appropriate time as shown in Table 2. The products isolated as described above.

### Spectroscopic Data of Representative Compounds.

#### **2-Amino-3-cyano-4-phenyl-7,7-dimethyl-5-oxo-4H-5,6,7,8-tetrahydrobenzo[b]pyran (4a),**

$^1\text{H}$  NMR (300 MHz,  $\text{CDCl}_3$ , ppm)  $\delta$  1.04 (s, 3H), 1.13 (s, 3H), 2.11-2.21 (m, 2H), 2.42 (s, 2H), 4.67 (s, 1H), 6.52 (brs, 2H,  $\text{D}_2\text{O}$  exchangeable), 7.14-7.42 (m, 5H);  $^{13}\text{C}$  NMR (75 MHz,  $\text{CDCl}_3$ , ppm)  $\delta$  26.32, 27.65, 31.24, 35.09, 39.08, 49.98, 59.74, 113.09, 118.42, 125.86, 126.63, 127.54, 142.68, 158.54, 162.32, 194.24; IR (KBr disc,  $\text{cm}^{-1}$ ): 3320, 3202, 2214, 1688, 1624, 1507, 1482, 1370.

#### **2-Amino-3-cyano-4-(4-nitro phenyl)-5-oxo-4H-5,6,7,8-tetrahydrobenzo[b]pyran (4d).**

$^1\text{H}$  NMR (300 MHz,  $\text{CDCl}_3$ , ppm)  $\delta$  2.10-2.20 (m, 2H), 2.41-2.55 (m, 2H), 2.80-2.88 (m, 1H), 2.93-3.00 (m, 1H), 5.68 (s, 1H), 6.09 (brs, 2H,  $\text{D}_2\text{O}$  exchangeable), 7.32 (d, 2H), 7.84 (d, 2H);  $^{13}\text{C}$  NMR (75 MHz,  $\text{CDCl}_3$ , ppm)  $\delta$  20.87, 27.98, 35.43, 37.61, 50.43, 61.21, 114.32, 118.76, 126.03, 126.68, 130.02, 142.02, 160.45, 163.18, 198.23; IR (KBr disc,  $\text{cm}^{-1}$ ): 3380, 3340, 2225, 1680, 1590, 1490, 1460, 1380.

**Ethyl 2-amino-3-cyano-6-methyl-4-(3-nitrophenyl)-4H-pyran-5-carboxylate (6d)**,  $^1\text{H}$  NMR (300 MHz,  $\text{CDCl}_3$ ),  $\delta$  1.12 (t, 3H), 2.41 (s, 3H), 4.05 (q, 2H), 4.58 (s, 1H), 4.69 (brs, 2H,  $\text{D}_2\text{O}$  exchangeable), 7.49 (m, 5H, ArH);  $^{13}\text{C}$  NMR (75 MHz,  $\text{CDCl}_3$ ),  $\delta$  12.90, 17.64, 37.75, 59.95, 63.50, 105.93, 117.33, 121.39, 121.55, 128.51, 133.01, 145.10, 147.47, 159.77, 156.95, 164.26; IR (KBr disc,  $\text{cm}^{-1}$ ): 3410, 3330 (s), 3220, 2987, 2190, 1670, 1530, 1340, 1060.

**Ethyl 2-amino-3-cyano-6-methyl-4-(4-methylphenyl)-4H-pyran-5-carboxylate (6f)**,  $^1\text{H}$  NMR (300 MHz,  $\text{CDCl}_3$ ),  $\delta$  1.27 (t, 3H), 2.31 (s, 3H), 2.36 (s, 3H), 4.03 (q, 2H), 4.41 (s, 1H), 4.54 (brs, 2H,  $\text{D}_2\text{O}$  exchangeable), 7.09-7.32 (d, 2H, ArH), 7.46-7.61 (d, 2H, ArH);  $^{13}\text{C}$  NMR (75 MHz,  $\text{CDCl}_3$ ); 13.90, 14.21, 18.37, 38.39, 60.20, 60.64, 108.12, 127.37, 128.40, 129.24, 129.90, 136.71, 156.55, 157.56, 165.96. IR (KBr disc,  $\text{cm}^{-1}$ ): 3410, 3330, 3220, 2190, 1690, 1610, 1580, 1260, 1060.

**6-Amino-3-methyl-5-cyano-4-(phenyl)-1,4-dihydropyrano[2,3-c]pyrazole (8a)**,  $^1\text{H}$  NMR (300 MHz,  $\text{DMSO-d}_6$ ):  $\delta$  1.77 (s, 3H), 5.16 (s, 1H), 7.28-7.48 (m, 10H), 7.78 (brs, 2H,  $\text{D}_2\text{O}$  exchangeable);  $^{13}\text{C}$  NMR (75 MHz,  $\text{CDCl}_3$ , ppm)  $\delta$  25.02, 40.43, 50.45, 59.13, 113.24, 118.67, 126.45, 126.06, 127.67, 128.03, 128.98, 129.14, 130.14, 140.05, 154.05, 162.34; IR (KBr disc,  $\text{cm}^{-1}$ ): 3420, 3330, 2200, 1620, 1590, 1480, 1380.

**6-Amino-3-methyl-5-cyano-4-(3-nitrophenyl)-1,4-dihydropyrano[2,3-c]pyrazole (8e)**,  $^1\text{H}$  NMR (300 MHz,  $\text{DMSO-d}_6$ , ppm):  $\delta$  1.79 (s, 3H), 5.16 (s, 1H), 6.05 (brs, 2H,  $\text{D}_2\text{O}$  exchangeable), 7.19-7.68 (m, 8H), 8.01 (s, 1H);  $^{13}\text{C}$  NMR (75 MHz,  $\text{DMSO-d}_6$ , ppm)  $\delta$  25.67, 41.12, 51.61, 61.05, 113.78, 119.14, 125.79, 126.54, 126.98, 127.32, 128.12, 128.67, 129.34, 130.78, 131.05, 140.67, 154.67, 159.89; IR (KBr disc,  $\text{cm}^{-1}$ ): 3420, 3310, 2198, 1618, 1598, 1568, 1490, 1386.

**6-Amino-3-methyl-4-(4-methoxyphenyl)-1,4-dihydro-pyrano[2,3-c]pyrazole-5-carbonitrile (10b)**,  $^1\text{H}$  NMR (300 MHz, DMSO- $d_6$ , ppm):  $\delta$  1.79 (s, 3H), 3.45 (s, 3H), 4.56 (s, 1H), 6.88 (brs, 2H, D<sub>2</sub>O exchangeable), 7.10 (d, 2H), 7.19 (d, 2H), 12.01 (s, 1H, D<sub>2</sub>O exchangeable);  $^{13}\text{C}$  NMR (75 MHz, DMSO- $d_6$ , ppm)  $\delta$  10.22, 35.17, 36.01, 57.64, 97.82, 121.31, 126.04, 128.64, 136.19, 136.07, 141.64, 155.22, 161.35; IR (KBr disc,  $\text{cm}^{-1}$ ): 3483, 3254, 2191, 1641, 1608, 1492, 1390.

## References

1. S. Ray, P. Manna, C. *Ultrason. Sonochem.*, 2015, **22**, 22.
2. M. Ashokkumar, *Ultrason. Sonochem.*, 2011, **18**, 864.
3. T. J. Mason, *Chem. Soc. Rev.*, 1997, 26, 443.
4. S. F. Wang, C. L. Guo, K. K. Cui, Y. T. Zhu, J. X. Ding, X. Y. Zou, Y. H. Li, *Ultrason. Sonochem.*, 2015, **26**, 81.
5. N. Ghaffari Khaligh, F. Shirini, *Ultrason. Sonochem.*, 2015, **22**, 397.
6. B. Maleki, *Org. Prep. Proced. Int.*, 2016, **48**, 303.
7. B. Maleki, H. Eshghi, A. Khojastehnezhad, R. Tayebee, S. Sedigh Ashrafi, G. Esmailian Kahoo, F. Moeinpour, *RSC Adv.*, 2015, **5**, 64850.
8. Md. Nasim Khan, S. Pal, S. Karamthulla, L.H. Choudhury, *RSC Adv.*, 2014, **4**, 3732.
9. J. Safaei Ghomi, S. Zahedi, *Ultrason. Sonochem.*, 2017, **34**, 916.
10. B. Maleki, M. Baghayeri, S. M. Vahdat, A. Mohammadzadeh, S. Akhoondi, *RSC Adv.*, 2015, **5**, 46545.

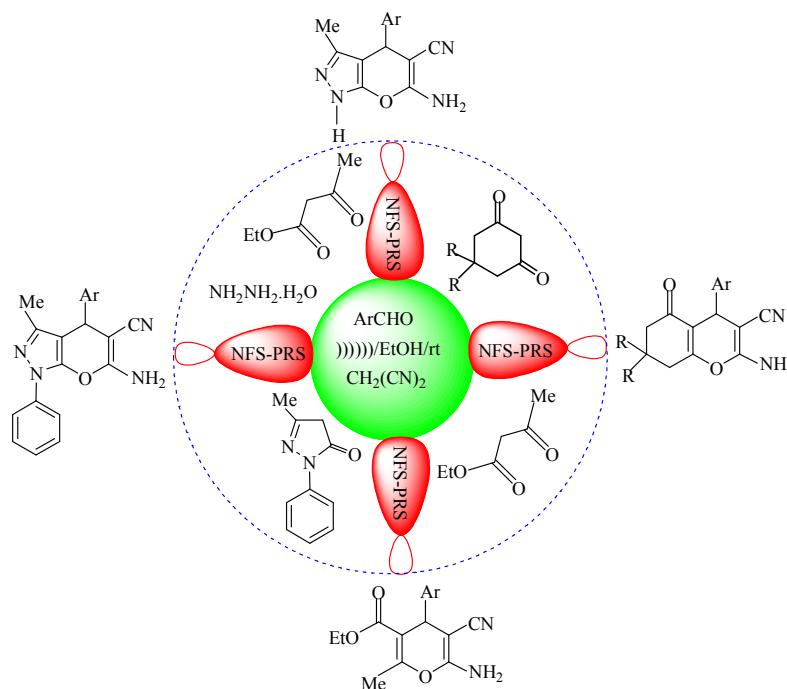
11. B. Maleki, E. Sheikh, E. Rezaei Seresht, H. Eshghi, S. Sedigh Ashrafi, A. Khojastehnezhad, H. Veisi, *Org. Prep. Proced. Int.*, 2016, **48**, 37.
12. B. Maleki, S. Barat Nam Chalki, S. Sedigh Ashrafi, E. Rezaei Seresht, F. Moeinpour, A. Khojastehnezhad, R. Tayebee, *Appl. Organomet. Chem.*, 2015, **29**, 290.
13. H. Veisi, A. Sedrpoushan, B. Maleki, M. Hekmati, M. Heidari, S. Hemmati, *Appl. Organomet. Chem.*, 2015, **29**, 834.
14. R. Tayebee, K. Savoji, M. Kargar Razi, B. Maleki, *RSC Adv.*, 2016, **6**, 55319.
15. B. Maleki, E. Rezaei-Seresht, Z. Ebrahimi, *Org. Prep. Proced. Int.*, 2015, **47**, 149.
16. B. Maleki, *Org. Prep. Proced. Int.*, 2016, **48**, 173.
17. B. Maleki, S. Babae, R. Tayebee, *Appl. Organomet. Chem.*, 2015, **29**, 408.
18. B. Maleki, *Collect. Czech. Chem. Commun.*, 2010, **76**, 27.
19. B. Maleki, E. Akbarzadeh, S. Babae, *Dyes Pigm.*, 2015, **123**, 222.
20. B. Maleki, R. Tayebee, Z. Sepehr, M. Kermanian, *Acta Chim. Slov.*, 2012, **59**, 814.
21. B. Maleki, S. Sedigh Ashrafi, R. Tayebee, *RSC Adv.*, 2014, **4**, 41521.
22. M. Rawat, V. Prutyantov, W. D. Wulff, *J. Am. Chem. Soc.*, 2006, **128**, 11044.
23. Kuzmina, J. A. K. Howard, M. Wenzel, K. Gloe, V. Lokshin, A. Samat, *J. Phys. Org. Chem.*, 2007, **20**, 469.
24. M. Kidwai, S. Saxena, M. K. R. Khan, S. S. *Bioorg. Med. Chem. Lett.*, 2005, **15**, 4295.
25. I. E. Soria-Mercado, A. Prieto-Davo, P. R. Jensen, W. J. Fenical, *J. Nat. Prod.*, 2005, **68**, 904.
26. R. R. Kumar, S. Perumal, P. Senthilkumar, P. Yogeewari, D. Sriram, *Bioorg. Med. Chem. Lett.*, 2007, **17**, 6459.

27. E. A. Hafez, M. H. Elnagdi, A. A. Elagamey, F. A. El-Taweel, *Heterocycles* 1987, **26**, 903.
28. D. Kumar, V. B. Reddy, S. Sharad, U. Dube, S. Kapur, *Eur. J. Med. Chem.*, 2009, **44**, 3805.
29. L. M. Wang, J. H. Shao, H. Tian, Y. H. Wang, B. Liu, *J. Fluorine Chem.*, 2006, **97**, 127.
30. J. L. Wang, D. Liu, Z. J. Zhang, S. Shan, X. Han, S. M. Srinivasula, C. M. Croce, E. S. Alnemri, Z. Huang, *Proc. Natl. Acad. Sci.*, 2000, **97**, 7124.
31. M. E. A. Zaki, M. H. A. Soliman, O. A. Hiekal, A. E. Z. Rashad, *Naturforsch C* 2006, **61**, 1.
32. A. D. Patil, A. J. Freyer, D. S. Eggleston, R. C. Haltiwanger, M. F. Bean, P. B. Taylor, M. J. Cranfa, A. L. Breen, H. R. Bartus, R. K. Johnson, R. P. Hertzberg, J. W. Westley, *J. Med. Chem.*, 1993, **36**, 4131.
33. C. S. Konkoy, D. B. Fick, S. X. Cai, N. C. Lan, J. F. W. Keana, Int. Appl. WO 0075123 2000; *Chem. Abstr.*, 2001, **134**, 29313a.
34. S. Wang, Q. Z. Qi, C. P. Li, G. H. Ding, S. H. Kim, *Dyes Pigm.*, 2011, **89**, 188.
35. Y. Suzuki, K. J. Yokoyama, *J. Am. Chem. Soc.*, 2005, **127**, 17799.
36. M. Esmailpour, J. Javidi, F. Dehghani, F. Nowroozi Dodeji, *RSC Adv.*, 2015, **5**, 26625.
37. S. Balalaie, M. Sheikh-Ahmadi, M. Bararjanian, *Catal. Commun.*, 2007, **8**, 1724.
38. D. M. Pore, K. A. Undale, B. B. Dongare, U. V. Desai, *Catal. Lett.*, 2009, **132**, 104.
39. S. Tabassum, S. Govindaraju, R. R. Khan, M. A. Pasha, *Ultrason. Sonochem.*, 2015, **24**, 1.
40. B. Maleki, S. Sedigh Ashrafi, *RSC Adv.*, 2014, **4**, 42873.
41. F. Shahbazi, K. Amani, *Catal. Commun.*, 2014, **55**, 57.

42. A. Azarifar, R. Nejat-Yami, M. Al-Kobaisi, D. Azarifar, *J. Iran. Chem. Soc.*, 2013, **10**, 439.
43. K. Tabatabaeian, H. Heidari, M. Mamaghani, N. O. Mahmoodi, *Appl. Organomet. Chem.*, 2012, **26**, 56.
44. B. Maleki, H. Eshghi, M. Barghamadi, N. Nasiri, A. Khojastehnezhad, S. Sedigh Ashrafi, O. Pourshiani, *Res. Chem. Intermed.*, 2016, **44**, 3071.
45. A. Khazaei, F. Gholami, V. Khakyzadeh, A. R. Moosavi-Zare, J. Afsar, *RSC Adv.*, 2015, **5**, 14305.
46. K. Ablajan, Li. Ju. Wang, Z. Maimaiti, Y. T. Lu, *Monatsh Chem.*, 2014, **145**, 491.
47. R. Y. Guo, Z. M. An, L. P. Mo, S. T. Yang, H. X. Liu, S. X. Wang, Z. H. Zhang, *Tetrahedron* 2013, **69**, 9931.
48. B. Maleki, S. Sheikh, *RSC Adv.*, 2015, **5**, 42997.
49. B. Maleki, S. Sheikh, *Org. Prep. Proced. Int.*, 2015, **47**, 368.
50. B. Maleki, N. Nasiri, R. Tayebee, A. Khojastehnezhad, H. A. Akhlaghi, *RSC Adv.*, 2016, **6**, 79128.
51. J. K. Rajput, P. Arora, G. Kaur, M. Kaur, *Ultrason. Sonochem.*, 2015, **26**, 229.
52. A. Moshtaghi Zonouz, I. Eskandari, D. Moghani, *Chem. Sci. Trans.*, 2012, **1**, 91.
53. A. Sánchez, F. Hernández, P. C. Cruz, Y. Alcaraz, J. Tamariz, F. Delgado, M. A. Vázquez, *J. Mex. Chem. Soc.*, 2012, **56**, 121.
54. N. G. Shabalala, R. Pagadala, S. B. Jonnalagadda, *Ultrason. Sonochem.*, 2015, **27**, 423.
55. G. Brahmachari, B. Banerjee, *ACS Sustain. Chem. Engin.*, 2014, **2**, 411.

56. A. Khojastehnezhad, M. Rahimizadeh, H. Eshghi, F. Moeinpour, M. Bakavoli, *Chin. J Catal.*, 2014, **35**, 376.
57. H. Eshghi, A. Khojastehnezhad, F. Moeinpour, M. Bakavoli, S. M. Seyadi, M. Abbasi, *RSC Adv.*, 2014, **4**, 39782.
58. H. Eshghi, A. Khojastehnezhad, F. Moeinpour, S. Rezaeian, M. Bakavoli, M. Teymouri, A. Rostami, K. Haghbeen, *Tetrahedron* 2015, **71**, 436.
59. A. Javid, A. Khojastehnezhad, M. M. Heravi, F. F. Bamoharram, *Syn. React. Inorg. Met. Org.*, 2012, **42**, 14.
60. A. Hafizi, A. Ahmadpour, M. M. Heravi, F. F. Bamoharram. *Petrol. Sci. Technol.*, 2014, **32**, 1022.
61. A. Gharib, M. Jahangir, M. Roshani, J. Scheeren, S. Mohadeszadeh, S. Lagzian, *Polish J. Chem. Technol.*, 2011, **13**, 5.
62. S. Wang, Z. Zhang, B. Liu, J. Li, *Catal. Sci. Technol.*, 2013, **3**, 2104.
63. Hamadi H, Kootia M, Afshari M, Ghiasifar Z, Adibpour N. *J. Mol. Catal. A: Chem.*, 2013, **373**, 25.
64. S. Vivekanandhan, M. Venkateswarlu, D. Carnahan, M. Misra, A. K. Mohanty, N. *Ceramic. Inter.*, 2013, 39, 4105.
65. H. Wang, W. Zhang, F. Zhang, Y. Cao, W. Su, *J. Magn. Magn. Mat.*, 2008, 320, 1916.

## Graphical abstract

Ultrasound Promoted Facile One Pot Synthesis of Highly Substituted Pyran Derivatives Catalyzed by Silica-Coated Magnetic NiFe<sub>2</sub>O<sub>4</sub> Nanoparticles-Supported H<sub>14</sub>[NaP<sub>5</sub>W<sub>30</sub>O<sub>110</sub>] Under Mild ConditionsBehrooz Maleki<sup>\*1</sup>, Mehdi Baghayeri<sup>1</sup>, Sedigheh Ayazi Jannat Abadi<sup>1</sup>, Reza Tayebee<sup>1</sup> and Amir Khojastehnezhad<sup>2</sup>

- ◆ Application of ultrasonic method as a green source of energy to reduce the reaction times compared to conventional processes.
- ◆ The catalyst was characterized using SEM, TEM, XRD, VSM, EDX and FT-IR.
- ◆ Silica-coated magnetic NiFe<sub>2</sub>O<sub>4</sub> nanoparticles-supported H<sub>14</sub>[NaP<sub>5</sub>W<sub>30</sub>O<sub>110</sub>] were used as magnetically separable catalyst for efficient synthesis of highly substituted pyran derivatives with minimum work up.
- ◆ Reusability and inexpensive nature of the catalyst.